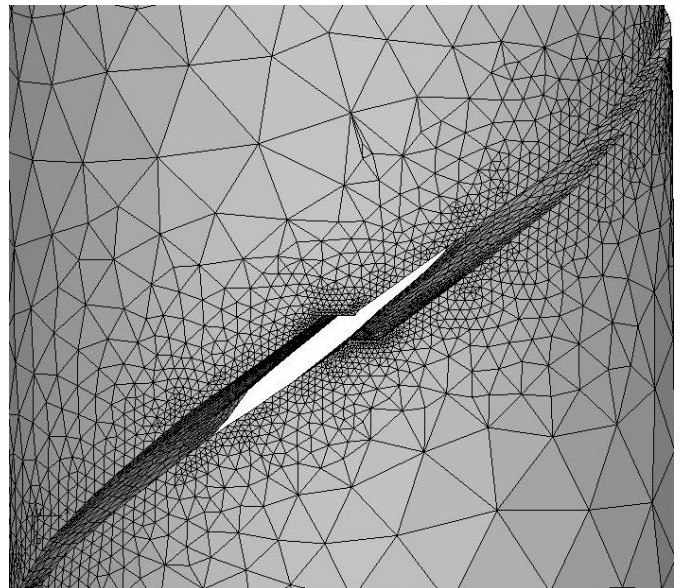


# FRANC3D

## Benchmark Examples



**Version 8.8**

Fracture Analysis Consultants, Inc  
<https://www.fracanalysis.com/>

Revised: Feb 2026

# Table of Contents

Table of Contents.....	2
1 Introduction.....	3
2 Interior Penny Shaped Crack in a Rectilinear Bar (Sneddon Solution).....	3
2.1 Crack Face Traction.....	7
2.2 M-integral versus Displacement Correlation SIFs.....	9
3 Internal, Inclined (45 degrees), Penny-Shaped Crack .....	11
4 Surface Ellipse Crack in a Plate – Raju-Newman Finite Element Solution .....	15
5 Through-Thickness Crack in a Plate.....	18
5.1 Through-Thickness Edge Crack .....	21
5.2 Middle-Through-Thickness (Center) Crack .....	24
6 Thick Plate with Middle Through Crack and Anisotropic Material Properties.....	26
6.1 Uniform Tension.....	28
6.2 Pure Shear .....	30
7 Corner Crack in a Plate with a Hole .....	31
8 Compact Tension Specimen .....	35
9 Circumferential Cracked Rod .....	38
10 Transverse Crack in a Pipe .....	40
11 Summary .....	42
References.....	43

# 1 Introduction

Benchmark examples and comparisons between analytical or handbook and FRANC3D stress intensity factors (SIF) are provided herein.

FRANC3D SIFs are computed using the M-integral approach, computed at crack front element mid-side nodes. Comparisons between the M-integral, VCCT and DC SIFs are included in the User's Guide, Chapters 11 and 12.

## 2 Interior Penny Shaped Crack in a Rectilinear Bar (Sneddon Solution)

An internal circular (penny-shape) crack is simulated in a rectilinear bar, Fig 2.1. The elastic modulus is 10,000 and Poisson's ratio ( $\nu$ ) is 0.0. The bar is constrained with simple supports. Unit traction is applied to the (left and right) end surfaces as indicated by the red arrows. ANSYS is used for the initial elastic stress analysis of the uncracked model, and the mesh information is archived to a *.cdb* file for use in FRANC3D.

We import the ANSYS FE model and use FRANC3D's submodeling tool to extract a local portion from the middle section of the bar. The crack is centered in the model and has a radius of 0.1 units, Fig 2.2.

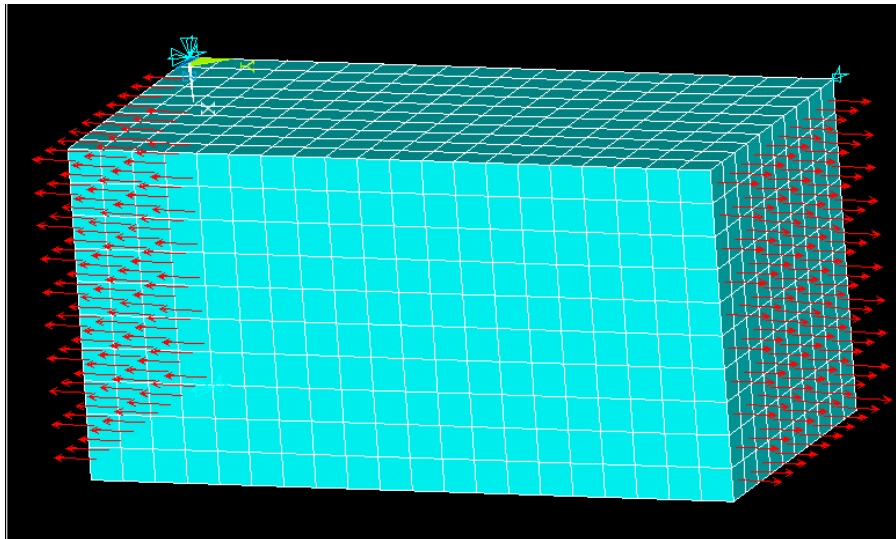


Figure 2.1 Rectilinear bar in ANSYS. It is 10 units long, 5 units wide and 5 units deep, with simple supports and unit uniform traction in the y-direction.

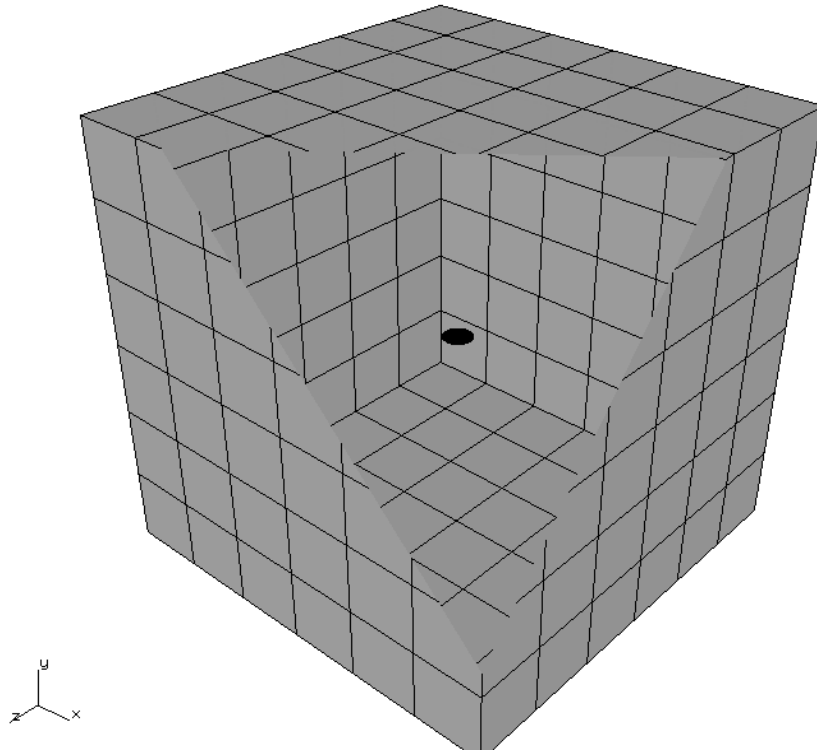


Figure 2.2 Internal penny-shaped crack with radius = 0.1 units.

The default crack front template radius is 0.01 units, Fig 2.3, with 8 elements around the crack front and 3 rings of elements (quarter-point wedge with two rings of bricks). About 33,500 elements are used; this includes the elements in the global portion of the model, which is not remeshed.

Mesh refinement can be used to study the accuracy of the SIFs. The number of rings of elements in the mesh template is increased from 3 to 6, the number of elements in each ring is increased from 8 to 16, and at the same time, the template element aspect ratio is decreased from 2 to 1. Increasing the number of rings reduces the size of the elements adjacent to the crack front while keeping the pyramid and tetrahedral elements the same distance away from the front. In addition to changing the template parameters, the crack surface mesh coarsening is turned off, Fig 2.4. About 161,500 elements are generated, including the elements in the global portion.

One could also try changing the advanced meshing parameters (see Section 5.2.9 in the Reference) or try other variations in template radius and template parameters.

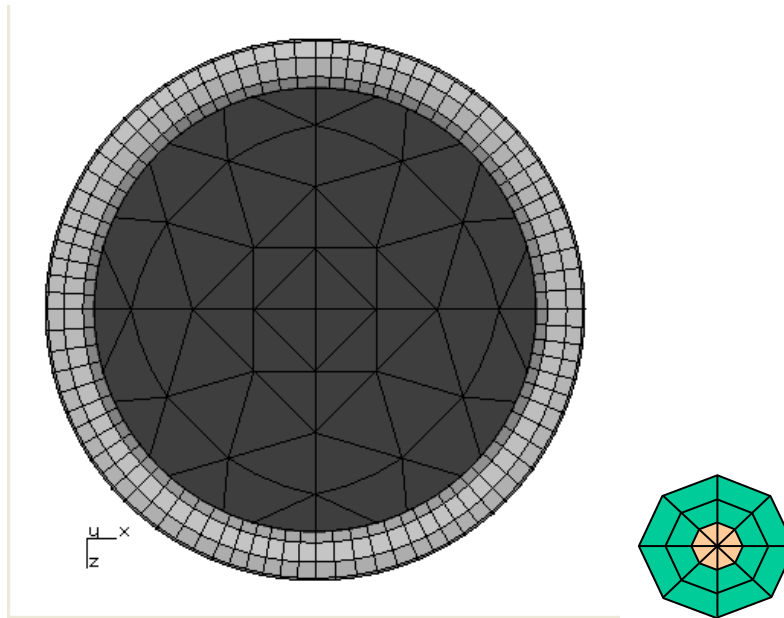


Figure 2.3. Default crack front template mesh, plan view and cross-section.

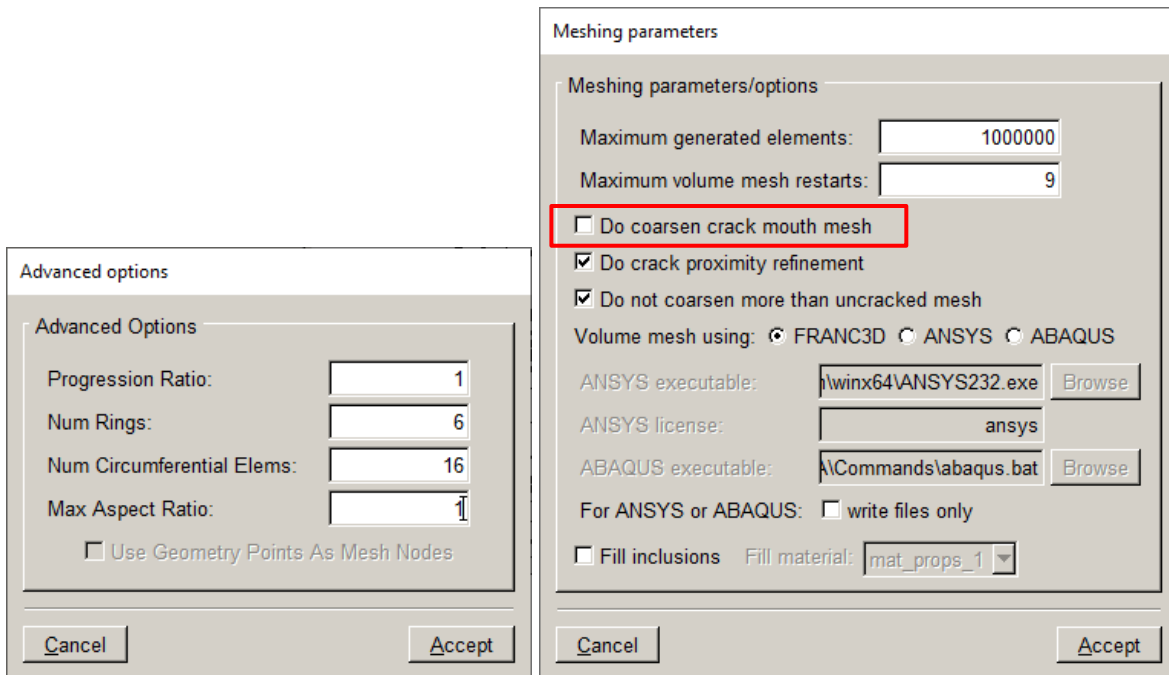


Figure 2.4. Template options (left) and meshing parameters (right); Do coarsen... is off.

The Mode I SIFs for the two analyses are shown in Fig 2.5. The % error (difference from the analytical solution) is shown in Fig 2.6.

The analytical solution for the Mode I SIF for this crack, in an infinite domain, was given by Sneddon (see Murakami, 1987) as:

$$K_I = 2\sigma\sqrt{\frac{a}{\pi}}$$
$$K_{II} = K_{III} = 0$$

The target value of  $K_I$  is 0.3568 and is constant along the crack front.

The mean value for the default mesh is 0.3582, and the mean difference from the analytical value is 0.4%. The mean value for the refined mesh is 0.3573, and the mean difference in this case is 0.13%.

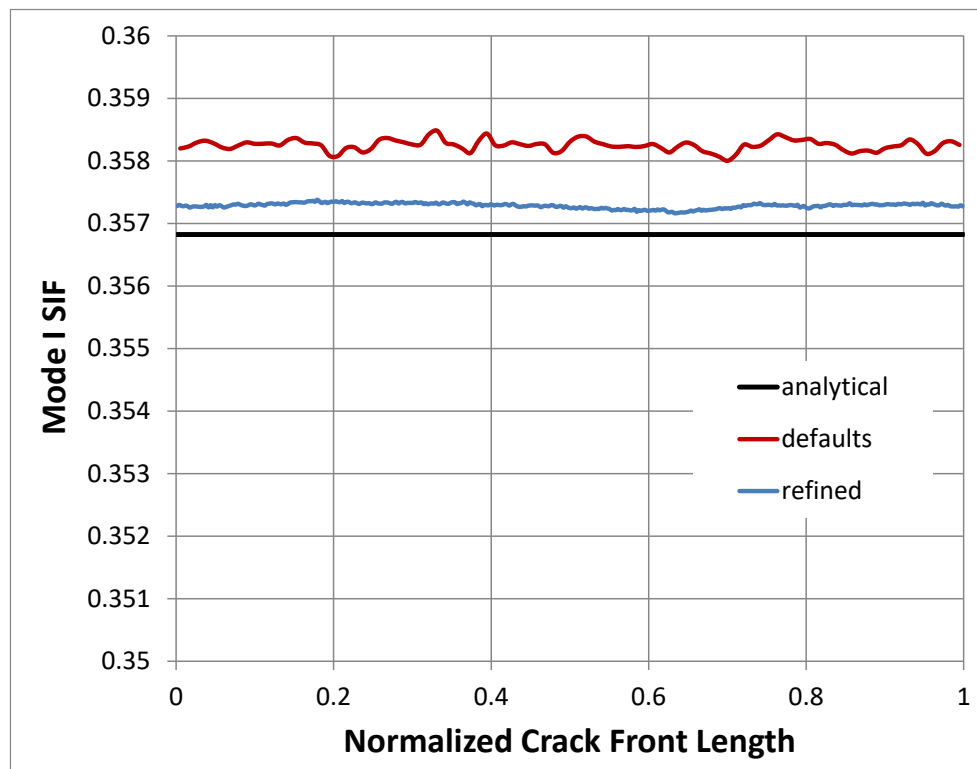


Figure 2.5 Mode I SIFs for the internal penny-shape crack.

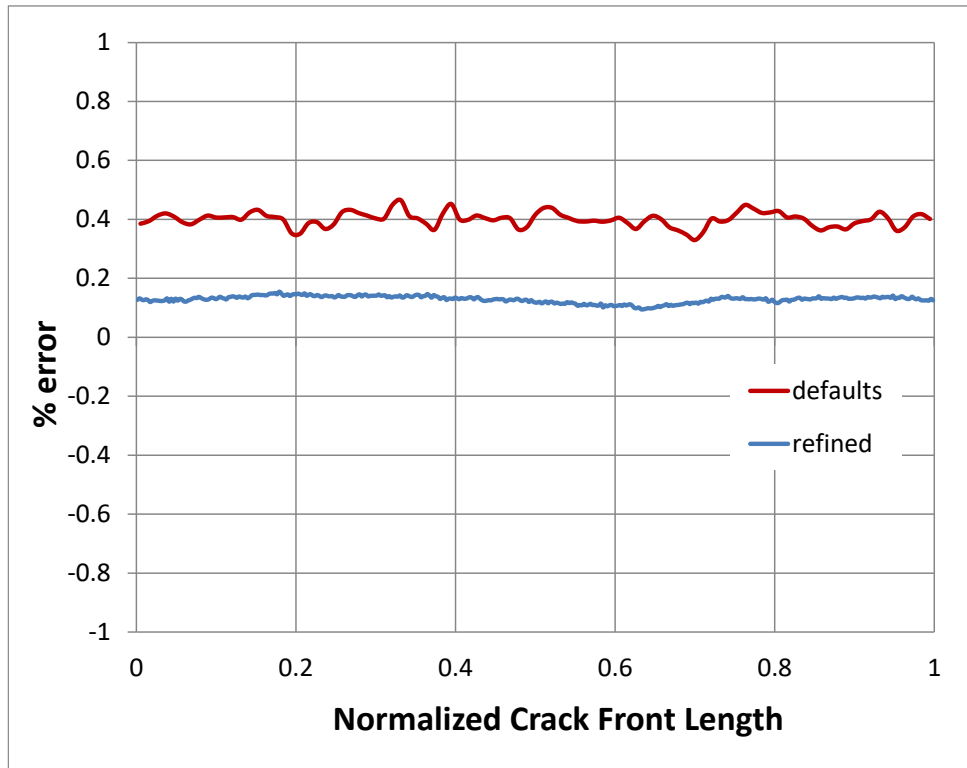


Figure 2.6 % error in Mode I SIFs for the internal penny-shape crack.

## 2.1 Crack Face Traction

FRANC3D allows one to apply crack face pressure or traction (CFT). The Tutorials use CFTs, so we use CFTs here to demonstrate that the computed SIFs are comparable to those for far-field loading.

The ANSYS FE model and crack geometry from Section 2.1 are used to compare the Mode I SIF solution for remote loading versus CFT. The far-field traction shown in Fig 2.1 is removed from the FE model and a constant unit crack face pressure is applied instead.

The Mode I SIFs are shown in Fig 2.7 and the % error (difference from reference solution) is shown in Fig 2.8. For the default mesh, the average Mode I SIF is 0.3574 and the average % error is 0.16. For the refined mesh, the average Mode I SIF is 0.3572 and the average % error is 0.11. These SIF values are nearly identical to the corresponding SIFs for far-field loading.

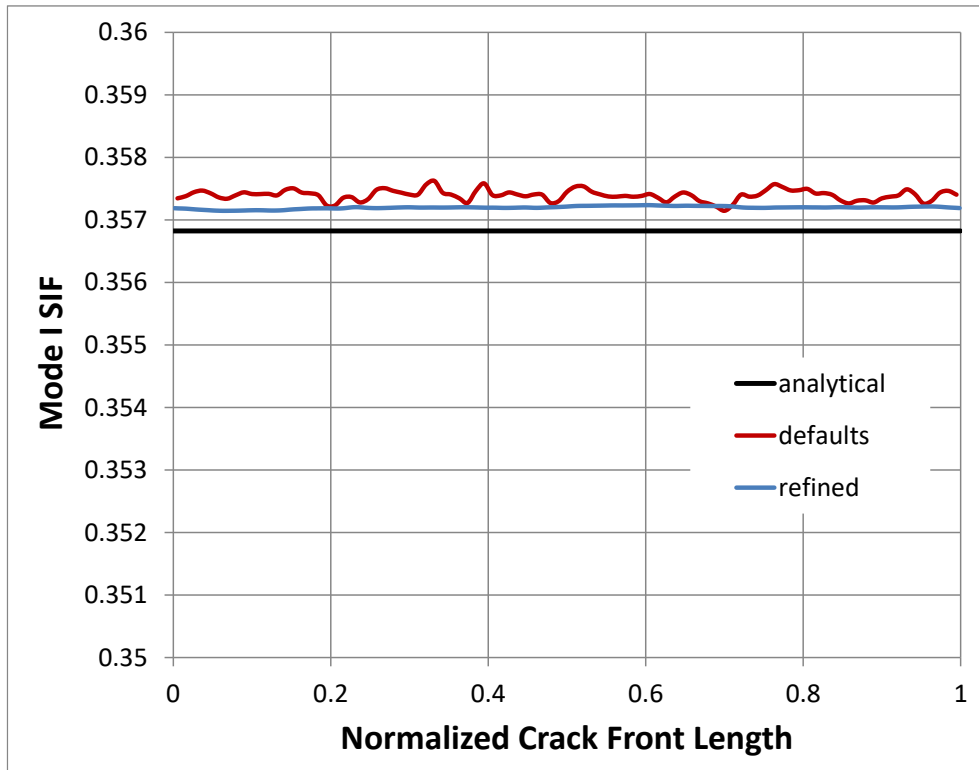


Figure 2.7 Mode I SIFs for the internal penny-shape crack with CFT.

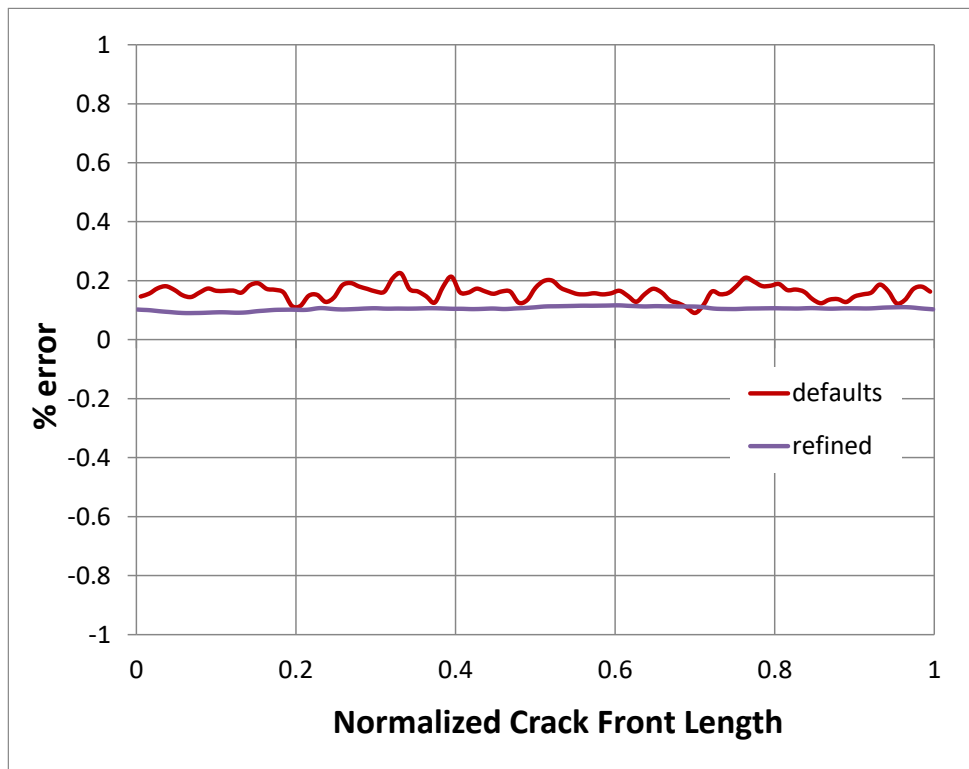


Figure 2.8 % error in Mode I SIFs for the internal penny-shape crack with CFT.

## 2.2 M-integral versus Displacement Correlation SIFs

FRANC3D allows one to compute SIFs using M-integral (MI), displacement correlation (DC) or virtual crack closure (VCCT) methods. Some of the Tutorials suggest comparing the MI SIFs with the DC SIFs. We do this here to show that the SIFs from both methods should be close. For the far-field applied load case, the MI and DC Mode I SIFs are plotted in Fig 2.9, and the % error is plotted in Fig 2.10.

The DC SIFs are slightly lower than the analytical solution for the default mesh and template parameters. For the refined mesh, the SIFs are close with average MI and DC Mode I SIFs of 0.3572 and 0.3575, respectively. The average % error is 0.105 and 0.186, respectively.

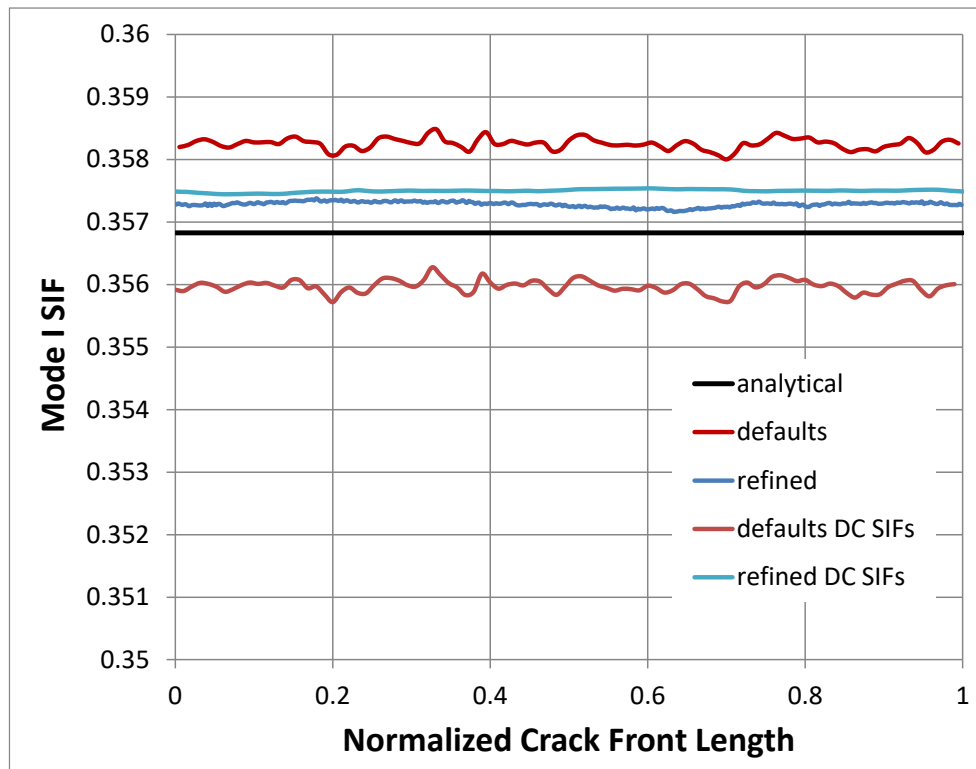


Figure 2.9 Mode I SIFs for the internal penny-shape crack.

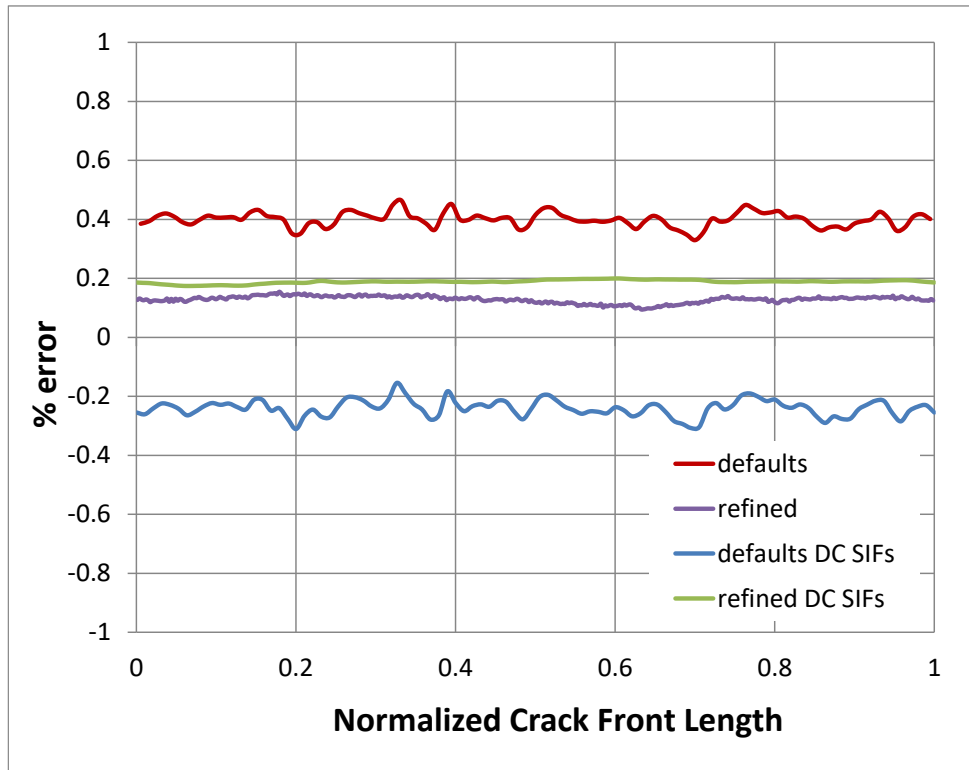


Figure 2.10 % error in Mode I SIFs for the internal penny-shape crack.

### 3 Internal, Inclined (45 degrees), Penny-Shaped Crack

A 10x5x5 block is used to model an infinite body containing a centered, internal, penny-shaped crack, with radius=0.125, and inclined at 45 degrees, Fig 3.1. The loading is far-field uniform tension equal to 1.0, and the material properties consist of an elastic modulus of 10,000 and a Poisson's ratio of 0.0. An ANSYS FE model is created and the corresponding *.cdb* file is used in FRANC3D; Fig 3.1 shows a local portion of the full model.

The default crack front template mesh is shown in Fig 3.2. The default template radius is 0.0125 units with 3 rings of elements (quarter-point wedge and 2 rings of bricks) and 8 elements in each ring. Based on the results in Section 2, we create a mesh using all the default settings, Fig 3.3, and then create a refined mesh using the same template radius but with 6 rings of 16 elements and an aspect ratio of 1. About 40,000 elements are generated for the entire model with the default settings, and about 188,000 elements are generated for the refined mesh.

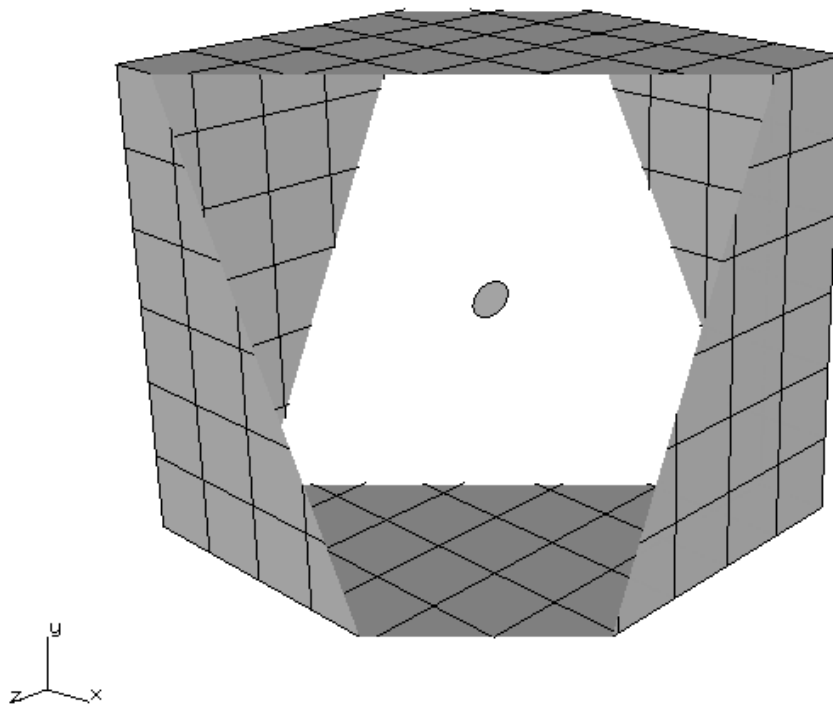


Figure 3.1 Internal, inclined at 45 degrees, penny-shaped crack in a rectilinear bar.

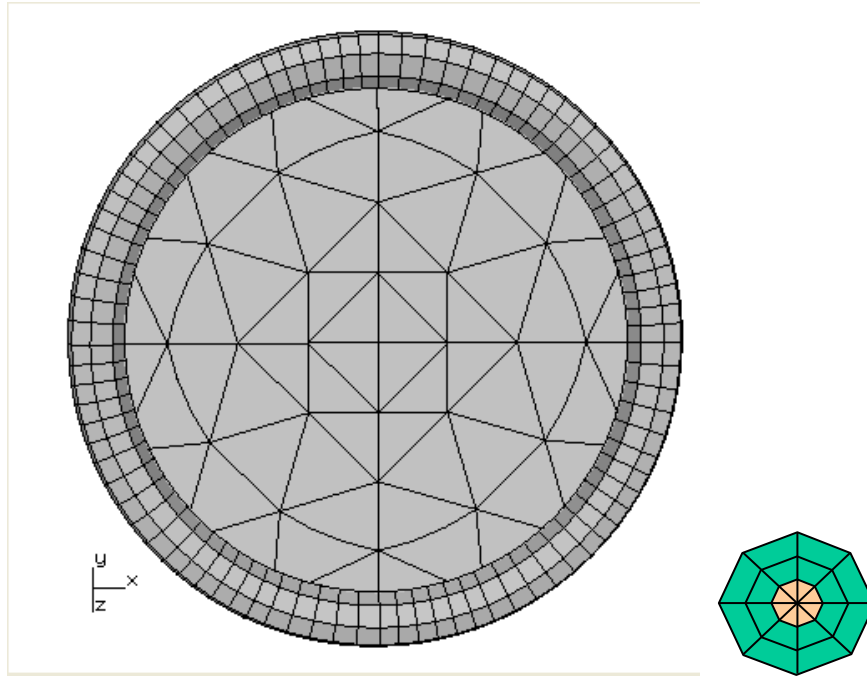


Figure 3.2 Default crack front template mesh.

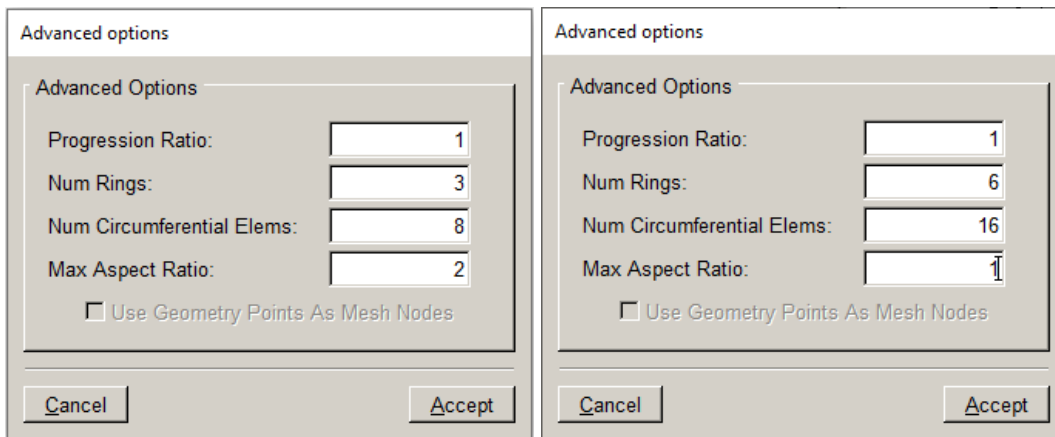


Figure 3.3 Default (left) and refined (right) crack front template settings.

The analytical values for Mode I, II and III SIFs for this configuration are available in Murakami (1987). Mode I SIF is constant at 0.200 along the crack front perimeter. Mode II SIF is zero at points A and B, Fig 3.4, and reaches a maximum (or minimum depending on the sign) at points C and D equal to 0.200 (or -0.200). Mode III SIF is zero at points C and D and reaches a maximum (or minimum) at points A and B equal to 0.200 (or -0.200). The equations for the three modes of SIF are:

$$K_I = \sigma \sin^2(\gamma) \sqrt{\pi r} (2/\pi)$$

$$K_{II} = \sigma \sin(\gamma) \cos(\gamma) \sin(\theta) \sqrt{\pi r} (2/\pi) (2/(2 - \nu))$$

$$K_{III} = \sigma \sin(\gamma) \cos(\gamma) \cos(\theta) \sqrt{\pi r} (2/\pi) (2/(2 - \nu)) (1 - \nu)$$

where  $\gamma$  is the angle of inclination (here 45 degrees),  $\theta$  is the position along the crack front,  $r$  is the crack radius.

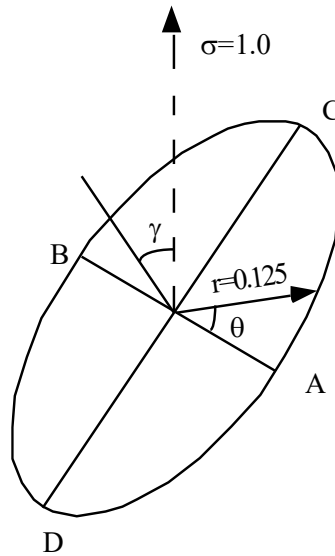


Figure 3.4 Inclined, penny-shaped crack subjected to uniform, remote tension.

All three SIF modes for the default mesh are shown in Fig 3.5. The mean value of Mode I is 0.2. The average error in Mode I SIF is 0.18%. The maximum absolute Mode II and Mode III values are 0.2 and 0.2. Fig 3.6 shows the same data for the refined mesh; there are no significant differences in the SIFs.

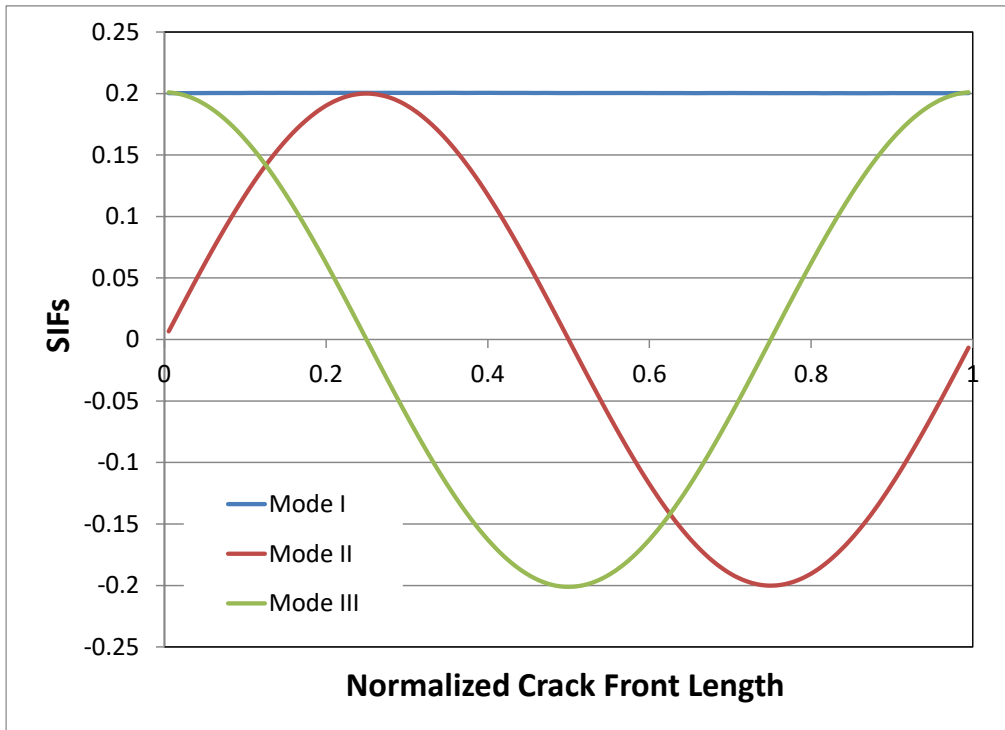


Figure 3.5 Mode I, II, and III SIFs along the crack front of an internal, inclined (at 45 degrees), penny-shaped crack under unit uniform uniaxial tension for the default template.

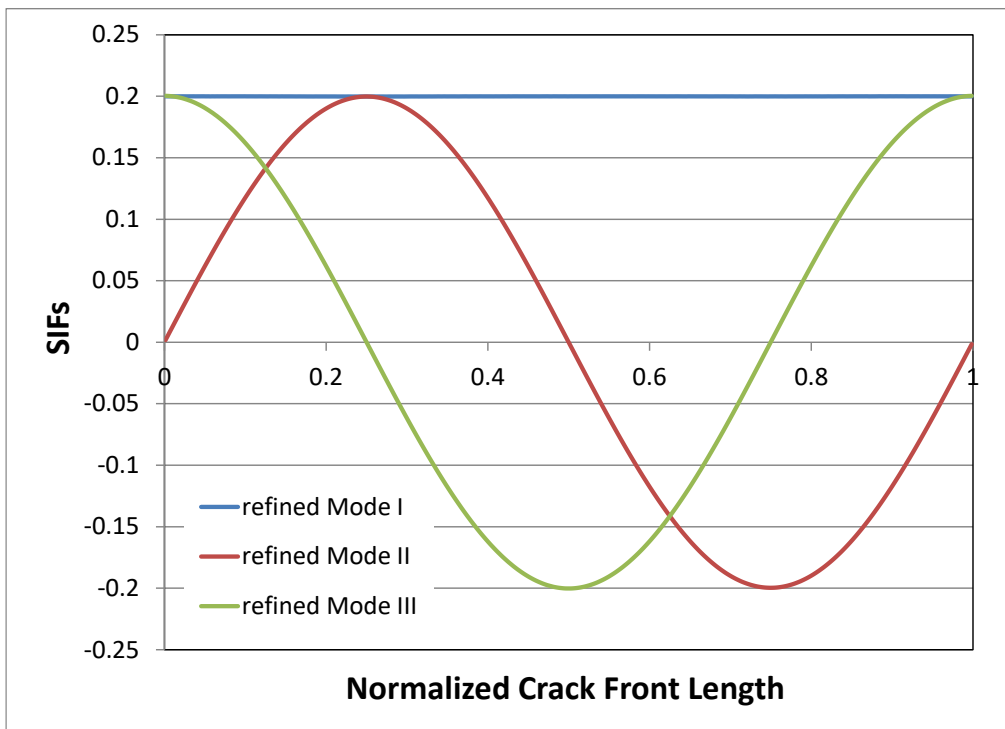


Figure 3.6 Mode I, II, and III SIFs along the crack front of an internal, inclined (at 45 degrees), penny-shaped crack under unit uniform uniaxial tension for a refined template mesh.

## 4 Surface Ellipse Crack in a Plate – Raju-Newman Finite Element Solution

The handbook solution, for a surface crack in a finite plate, was developed by Raju and Newman (1979; 1986); the reported accuracy is within 5%. Typical plate dimensions are depicted in Fig 4.1. The loading consists of uniform unit traction and simple constraints.

A FE model of the plate was created with dimensions:  $H=4$ ,  $W=4$ ,  $t=2$ . A crack, with dimensions:  $a=0.8$  and  $c=0.8$ , is inserted, Fig 4.2. The default crack front template, Fig 4.3, has a radius of 0.08 units, and 8 circumferential elements in 3 rings (quarter-point wedge and 2 rings of bricks) with an aspect ratio of 2. About 21,000 elements were generated for the entire model.

Based on the results from Section 2, we increase the number of rings in the template to 6, increase the number of elements in each ring to 16, and set the aspect ratio to 1. We also turn off the Do coarsen... mesh flag in the meshing parameters dialog. About 110,000 elements are generated for the entire model with these settings.

A third mesh is created by reducing the template radius to 0.04, with the refined mesh and template settings described above. About 231,000 elements are generated for the entire model with these settings.

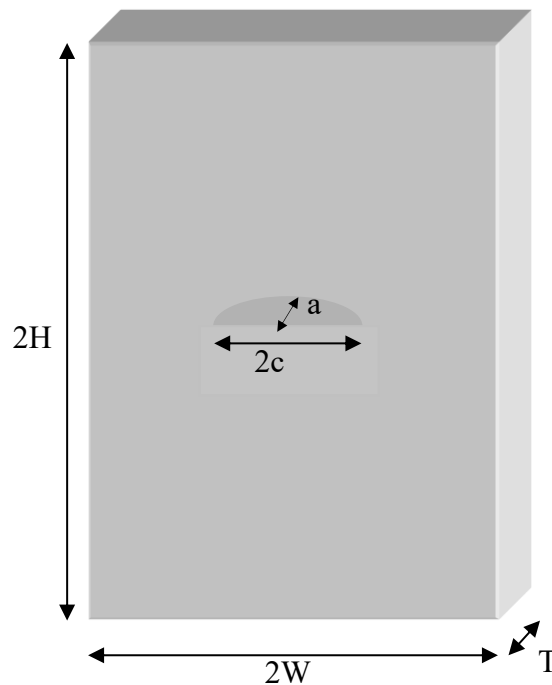


Figure 4.1 Raju/Newman surface crack in a plate model configuration.

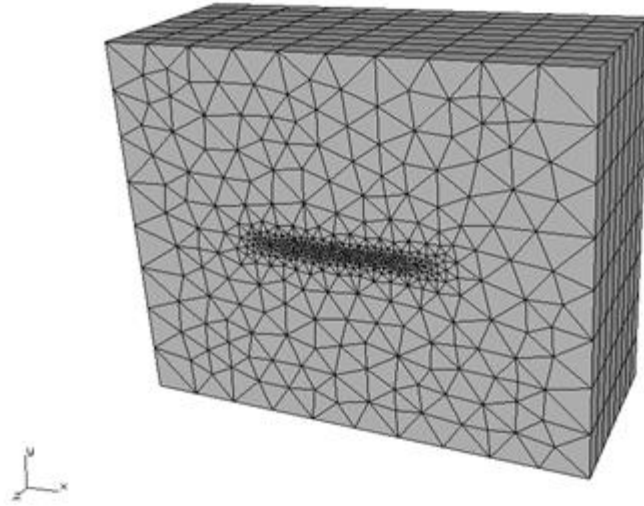


Figure 4.2 FRANC3D model of Raju-Newman surface crack in a plate.

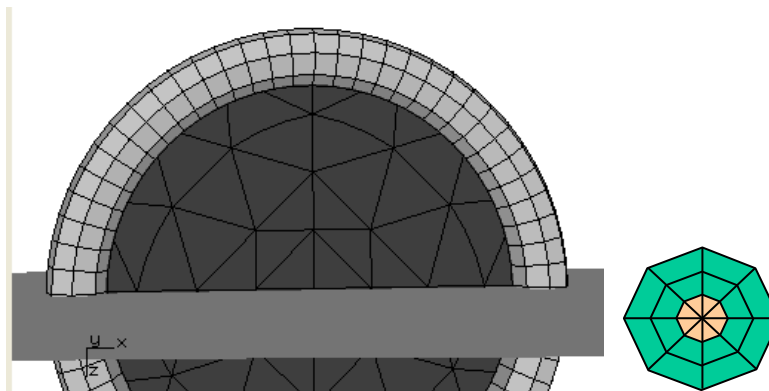


Figure 4.3 Default crack front template mesh for a half-penny surface crack.

The Mode I SIFs for the default mesh are plotted in Fig 4.4. There are some differences in Mode I SIFs, especially near the free surface; the difference is about 3%. At the mid-point, the difference is about 0.32%.

The refined mesh captures a drop in Mode I SIF at the surface, Fig 4.5, but the rest of the values are similar to the default mesh values. For the most refined mesh, with a template radius of 0.04, the difference at the free surface between the FRANC3D and Raju/Newman values is 0.04%, and the difference at the midpoint is about 0.8%.

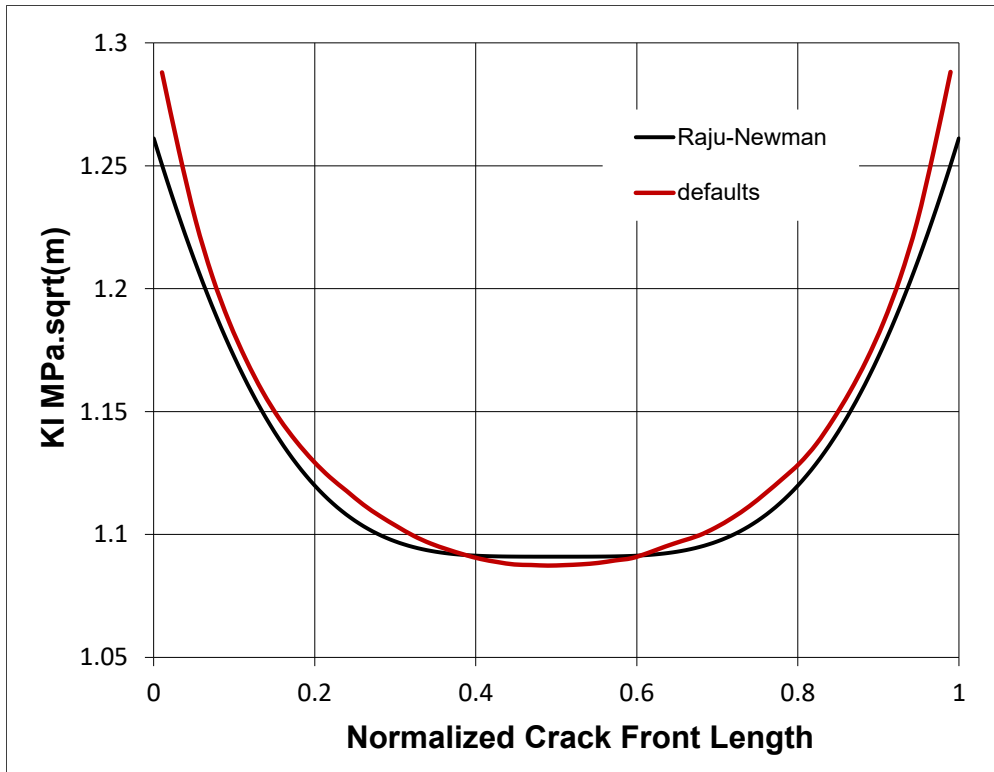


Figure 4.4 Raju-Newman surface crack in a plate – Mode I SIFs.

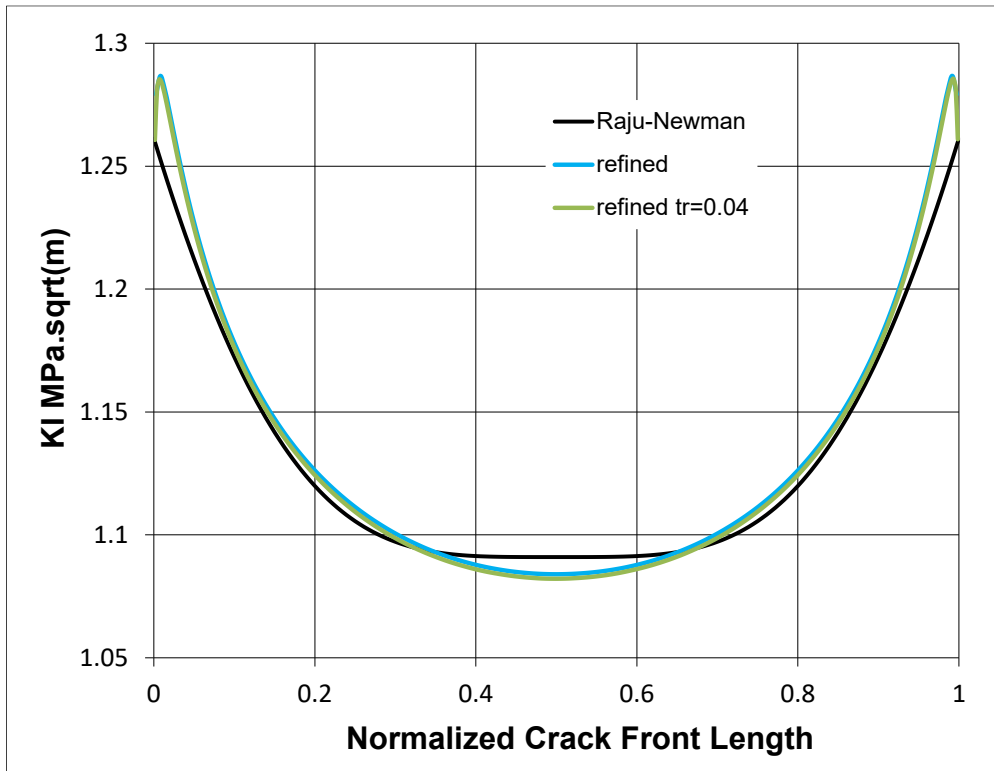


Figure 4.5 Raju-Newman surface crack in a plate – Mode I SIFs.

## 5 Through-Thickness Crack in a Plate

A through-thickness edge crack in a plate and a middle-through-thickness crack in a plate are standard benchmark problems. The model, Fig 5.1, is a 10x5x5 plate, and the boundary conditions consist of uniform traction and simple displacement constraints. The elastic modulus is  $3.0e7$  and Poisson's ratio is 0.30. The top and bottom surfaces of the plate have uniform unit traction.

Two sets of boundary conditions are applied to simulate a through-thickness edge crack and a middle-through-thickness crack. For the first case, only simple constraints are applied to prevent rigid body motion. For the second case, rollers in the x-direction (to use symmetry) are applied to the surface where the crack is inserted.

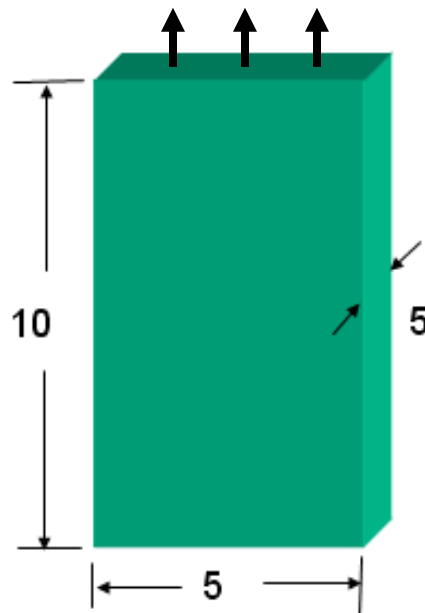


Figure 5.1 Plate model.

A crack of 0.5 units is inserted on the left side of the plate. The crack is defined to be slightly larger than the desired dimensions to make sure it intersects the model surface correctly, Figs 5.2-5.3. The default template radius (0.055) is based on the short dimension, which is 0.55; we change that to 0.05, Fig 5.4. For edge cracks that are shallow, it is usually best to turn off the Do coarsen..., Fig 5.5. All other template settings are left at the default values. The cracked meshed local model portion is shown in Fig 5.6.

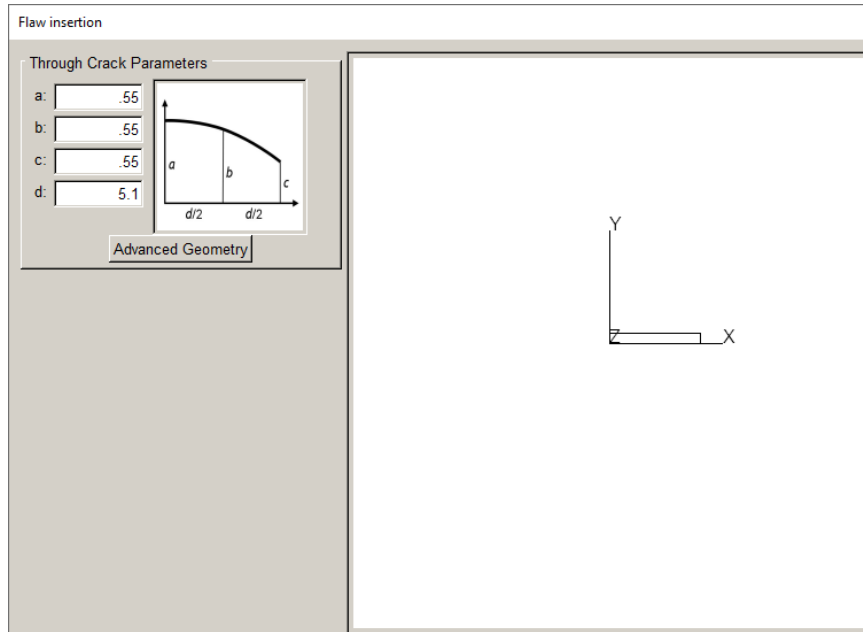


Figure 5.2 Edge crack dimensions.

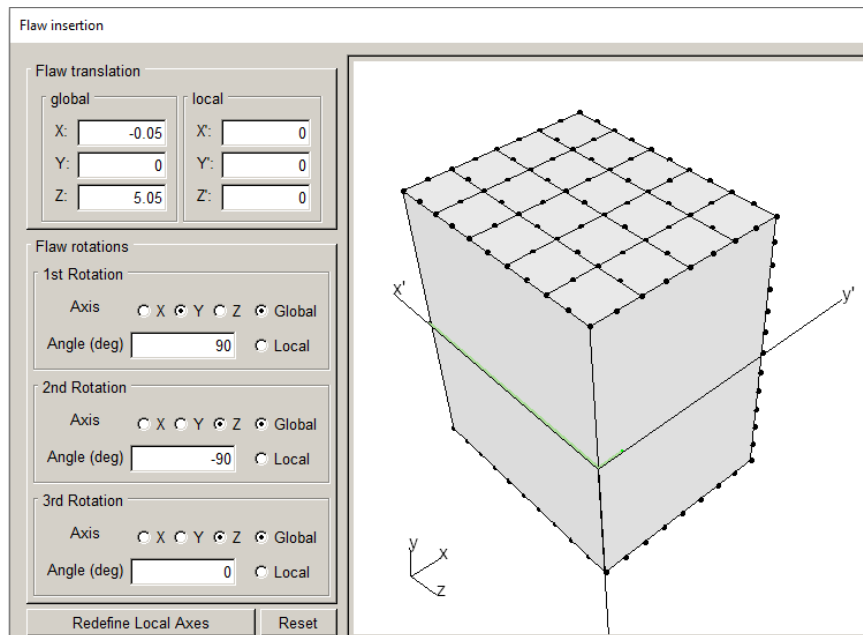


Figure 5.3 Edge crack location and orientation.

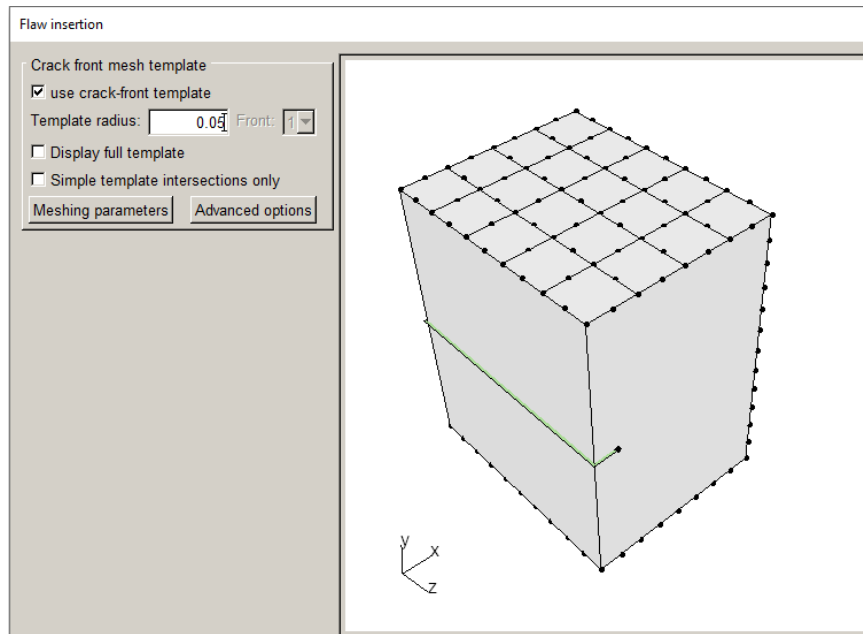


Figure 5.4 Edge crack template radius for the default template mesh.

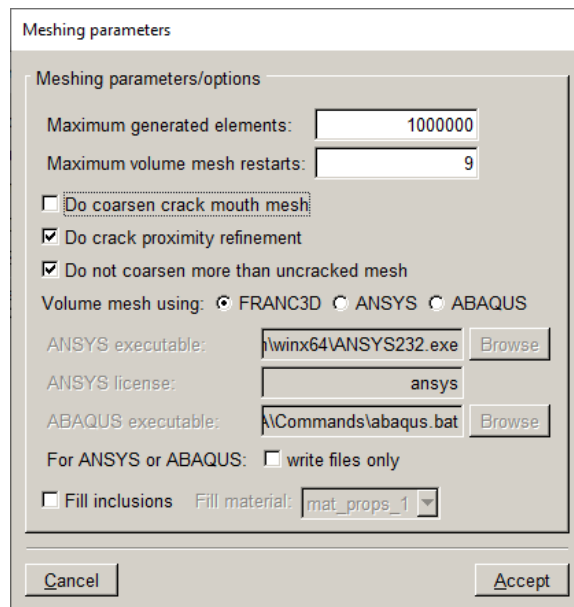


Figure 5.5 Edge crack meshing parameters.

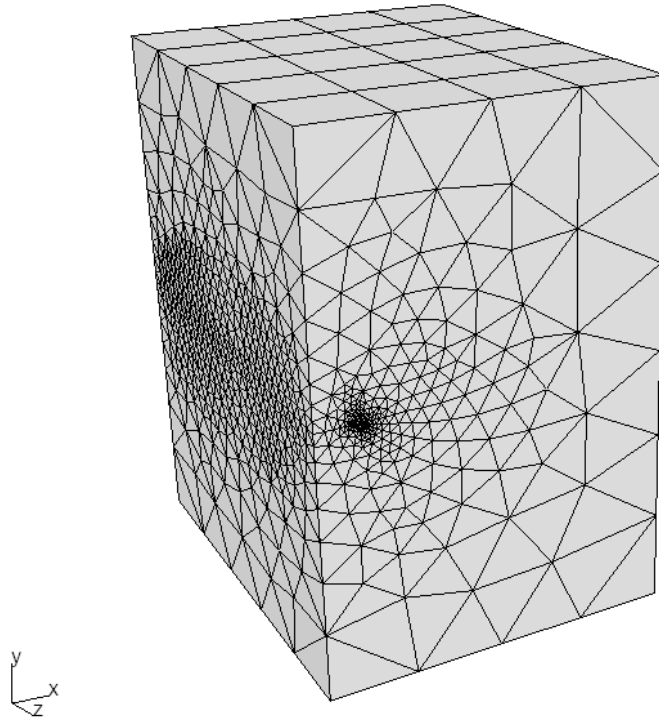


Figure 5.6 Local model portion with edge crack of length 0.5 units.

## 5.1 Through-Thickness Edge Crack

The default template radius is 0.05 units with 8 rings around the crack front and 3 rings of elements (quarter-point wedge and 2 rings of bricks). A refined mesh is created by increasing the number of element rings to 6, with 16 elements in each ring, and by setting aspect ratio to 1.

These settings are used for both the edge crack and the center crack (in the next section). About 52,000 elements are generated for the default edge crack mesh, and about 287,000 elements are generated for the more refined model.

The handbook 2D solution for the edge crack is given by the equation (Murakami, 1987):

$$K_I = \sigma \sqrt{\pi a} F_I(\alpha)$$

The correction factor is:

$$\alpha = \frac{a}{w}$$

$$F_I(\alpha) = (1.12 - 0.231\alpha + 10.55\alpha^2 - 21.72\alpha^3 + 30.39\alpha^4)$$

for  $\frac{a}{w} \leq 0.6$ .  $K_{II} = K_{III} = 0$ .

In this model,  $a=0.5$  and  $w=5$ , so the correction factor is 1.1837. The handbook  $K_I$  value is 1.484. The FRANC3D SIFs, which are affected by the Poisson's ratio, are shown in Fig 5.7. The defaults and refined meshes produce comparable results, but there is more numerical noise in the defaults mesh.

To eliminate the variation in SIFs through the thickness, we can either set Poisson's ratio to zero or constrain the model surfaces normal to the crack front. If we add constraint on the z-surfaces to simulate plane strain conditions, the average Mode I SIF value for the default mesh is 1.486, and for the refined mesh it is 1.489, Fig 5.8. The handbook solution is 1.484. The average difference between the FRANC3D Mode I SIF value and the handbook value is 0.16% and 0.4%, for the default and refined meshes, respectively.

If we set Poisson's ratio to zero, the Mode I SIFs are almost the same as for the constrained model, Fig 5.9; there is slightly less variation along the front.

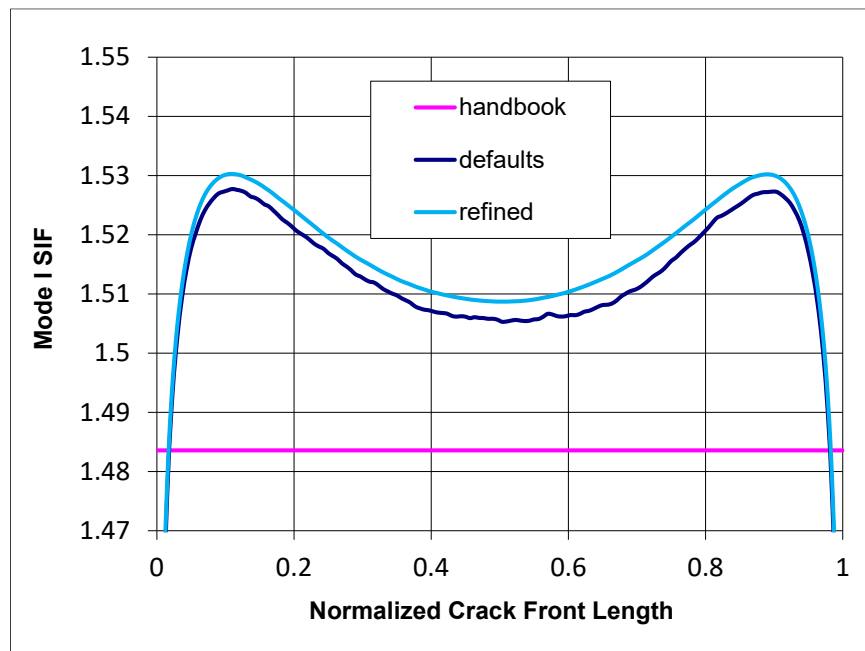


Figure 5.7 Mode I SIF values for edge crack.

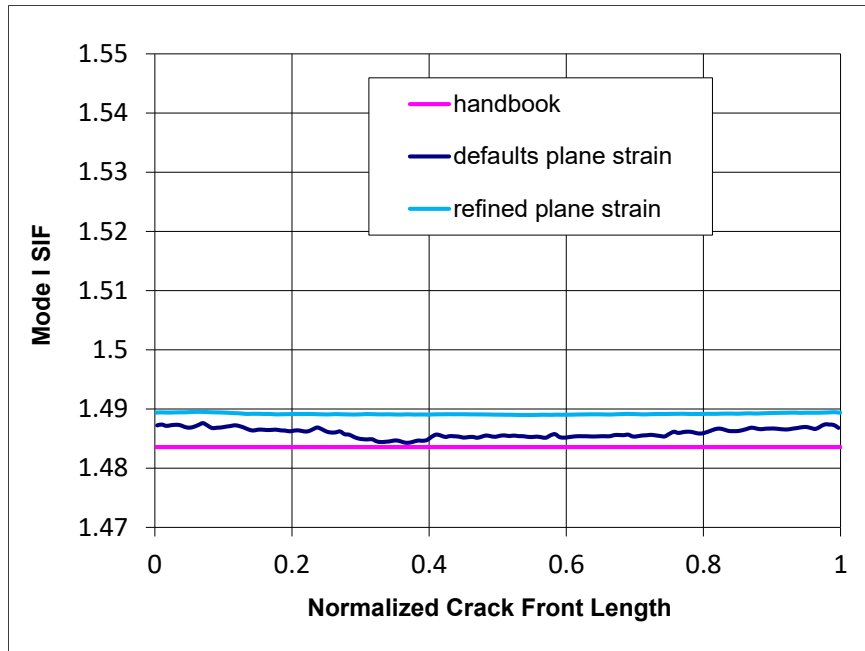


Figure 5.8 Mode I SIF values for edge crack with z-constraints.

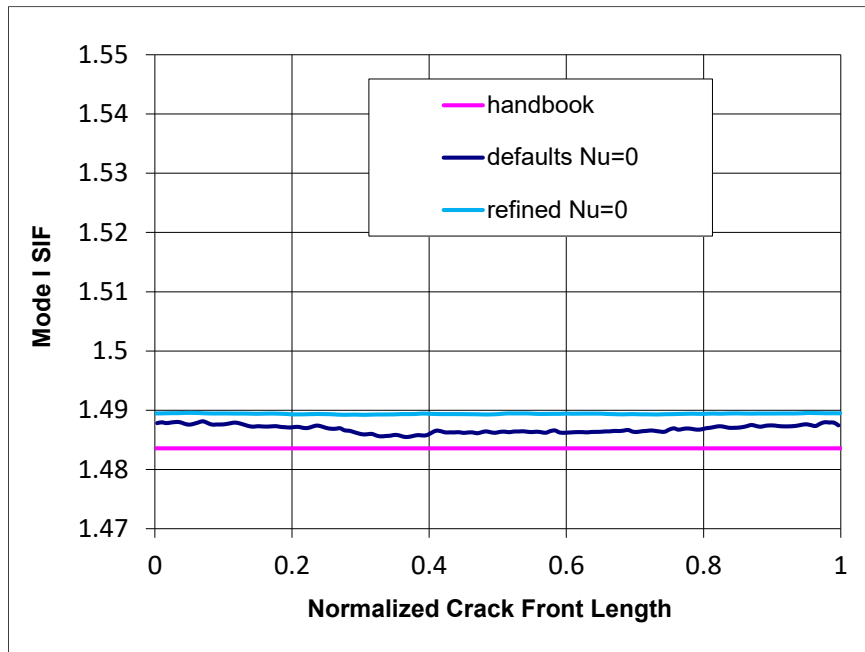


Figure 5.9 Mode I SIF values for edge crack with Poisson's ratio set to zero.

## 5.2 Middle-Through-Thickness (Center) Crack

The handbook 2D solution for Mode I SIF for the center crack is given in Murakami (1987). The equations are:

$$K_I = \sigma \sqrt{\pi a} F_I(\alpha, \beta)$$
$$\alpha = \frac{2a}{w}, \beta = h/W$$

The parameters  $h$ ,  $W$ , and  $a$  are depicted in Fig 5.10. For this model, the correction factor,  $F_I$ , is 1.014, so the handbook value of Mode I SIF is 1.271.

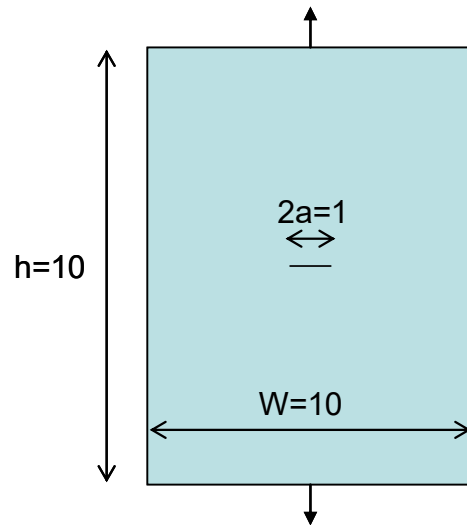


Figure 5.10 Center cracked plate under remote tension.

### 5.2.1 Symmetry Boundary Conditions

Symmetry boundary conditions are applied to the surface, normal to the  $x$ -axis at  $x=0$ , in the uncracked FE model, Fig 5.11. When we import the FE model into FRANC3D, we retain the displacement boundary conditions without retaining the associated nodes and mesh facets. FRANC3D transfers the constraints after crack insertion and remeshing. We could have doubled the plate geometry and redefined the crack geometry to create a model as shown in Fig 5.10, but symmetry reduces the model size.

When we write the cracked FE model file, all transferred boundary conditions are included. The symmetry boundary conditions on the surface where the crack is inserted can be verified using the FE pre-processor. Fig 5.11 shows the cracked symmetry model, without the  $z$ -constraint normal to the crack front.

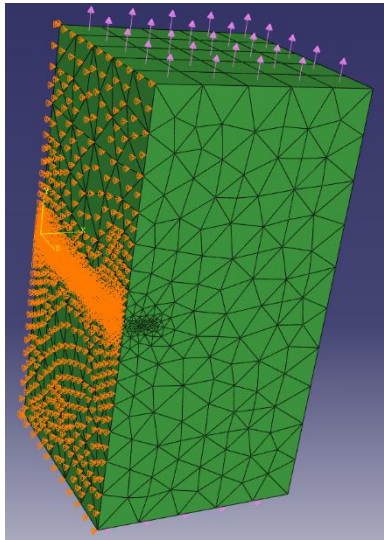


Figure 5.11 Boundary conditions shown in ABAQUS CAE for middle-crack model.

The FRANC3D Mode I SIF values are plotted in Fig 5.12 for both the default and refined meshes. The model is neither plane strain nor plane stress. If we set Poisson's ratio to zero to simulate plane strain conditions, the average Mode I SIF value for plane strain conditions is 1.268, Fig 5.13, for both meshes. The average difference between the FRANC3D Mode I SIF value and the handbook value is 0.23% and 0.1% for the default and refined meshes, respectively.

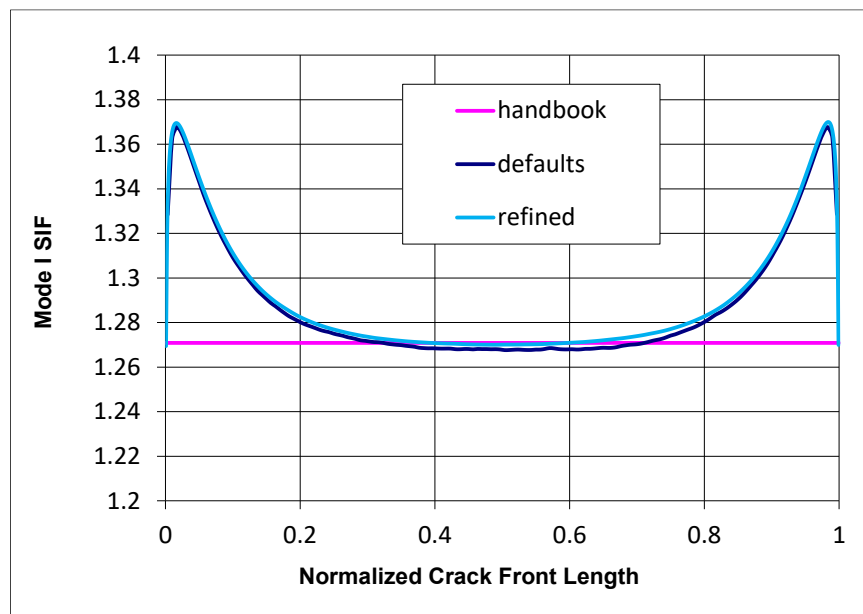


Figure 5.12 Mode I SIF values for middle-through crack.

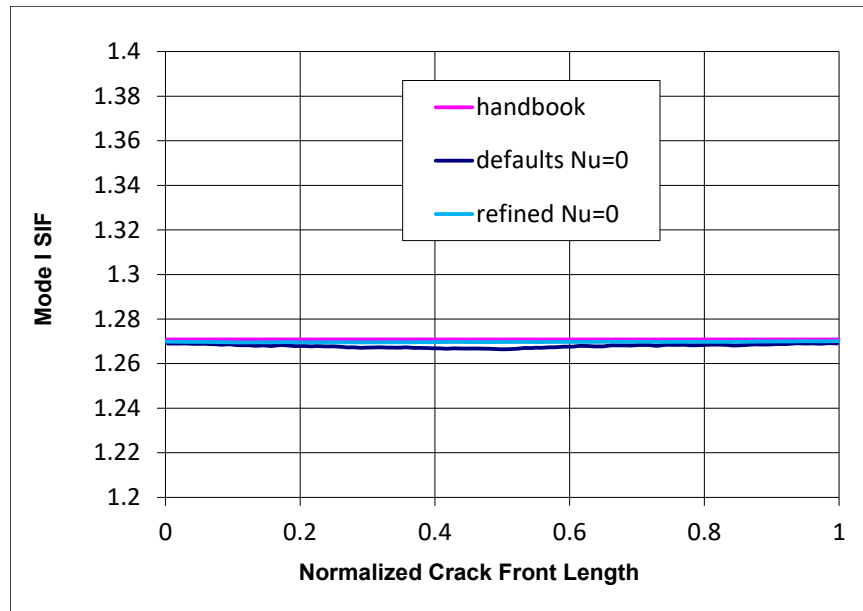


Figure 5.13 Mode I SIF values for middle-through crack.

## 6 Thick Plate with Middle Through Crack and Anisotropic Material Properties

A ‘thick plate’ model is used to verify that FRANC3D produces accurate stress intensity factors using the M-Integral for isotropic and anisotropic material properties (Banks-Sills *et al.*, 2007).

Two different sets of boundary conditions are used with this model: 1) uniform tension and 2) simple shear. The outer portion of the model is shown in Fig 6.1; the mesh is retained for the boundary conditions and for the cut-surfaces. The inner portion of the model is shown in Fig 6.2 with a crack inserted.

The original plate is 30x30x15 units and the through-crack is 2 units wide; plane strain conditions are approximated along the crack front in the middle of the plate. The material properties are provided in Table 1.

The plate is first analyzed with uniform tension and simple supports, Fig 6.3.

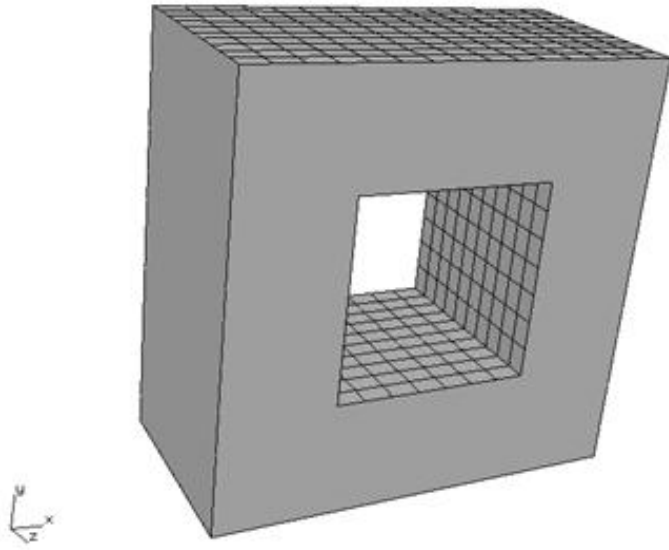


Figure 6.1: Outer portion of the thick plate model with tension boundary conditions.

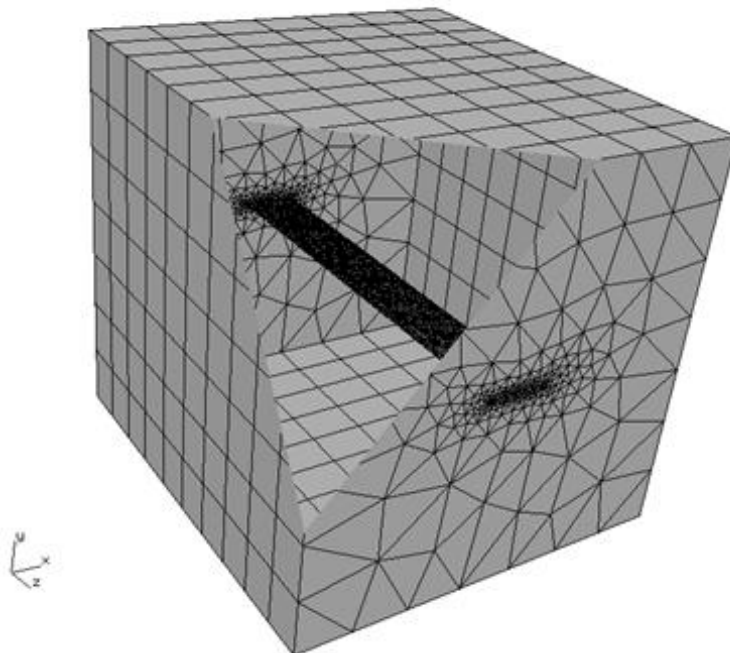


Figure 6.2 Thick plate inner portion with a middle through crack.

Table 1: Material Properties

	$E_x, E_y, E_z$	$\nu_{xy}, \nu_{yz}, \nu_{xz}$	$G_{xy}, G_{yz}, G_{xz}$
isotropic	950, 950, 950	0.3, 0.3, 0.3	
orthotropic	950, 950, 2400	0.45, 0.3, 0.3	328, 231, 231

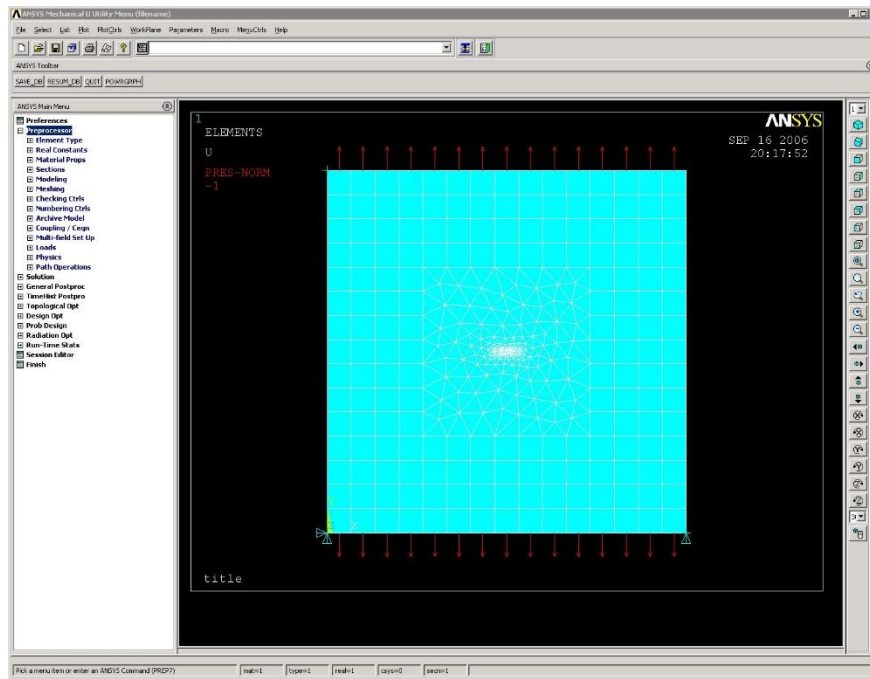


Figure 6.3 Thick plate with middle through crack; tension and simple constraints in ANSYS.

## 6.1 Uniform Tension

The template radius is 0.1 for both crack fronts, with 6 rings and 16 elements in each ring and an aspect ratio of one. The Do coarsen... flag is turned off. The stress analysis is done with ANSYS. The deformed shape with maximum principal stress contours is shown in Fig 6.4.

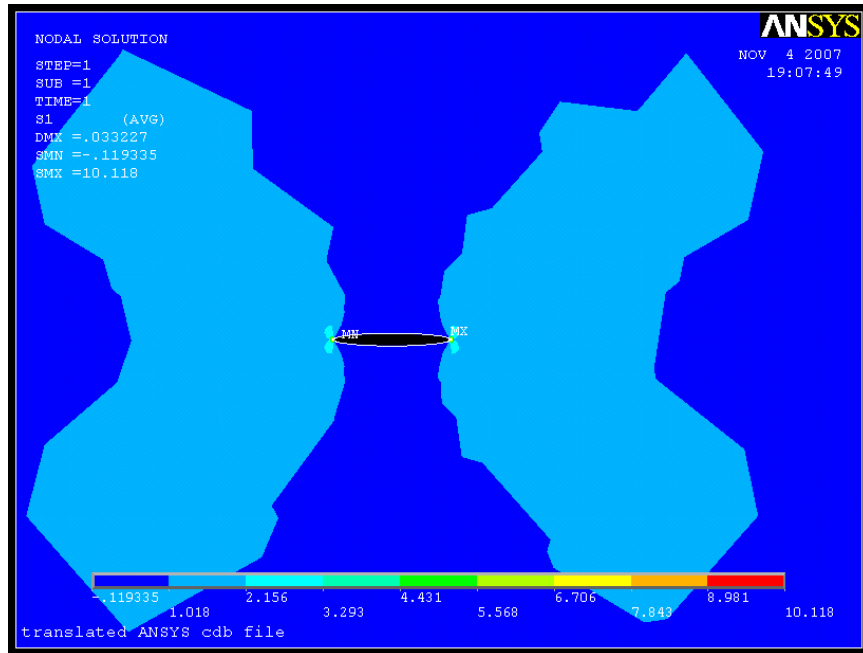


Figure 6.4 Thick plate deformed crack with maximum principal stress contours.

The analytical plane strain solution for Mode I SIF for the isotropic case under uniform tension is defined as:

$$K_I = \sigma \sqrt{\pi a}$$

where  $\sigma=1$  and  $a=1$ , resulting in  $K_I=1.772$ . The SIFs are plotted in Fig 6.5.

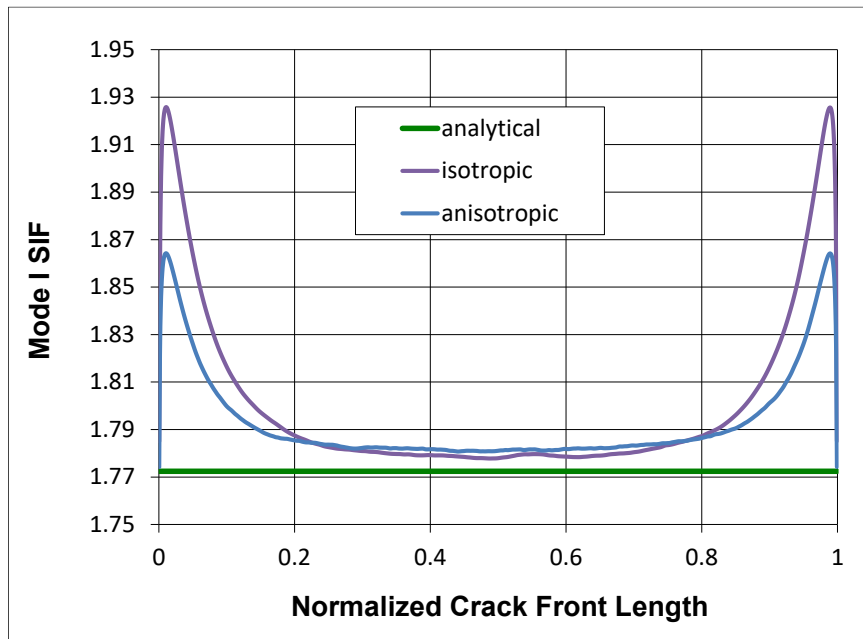


Figure 6.5 Mode I SIFs for thick plate under uniform tension for isotropic and anisotropic material properties.

## 6.2 Pure Shear

The second set of boundary conditions represents pure shear; Fig 6.6 shows the deformed shape of the original uncracked plate. The same crack front template and meshing parameters from Section 6.1 are used. The Mode II SIFs for pure shear are plotted in Fig 6.7; the Mode I SIFs are zero.

Note that the application of pure shear in ANSYS requires the use of surface effect elements and the shear is applied in the element coordinate system. The outer portion of the model was retained as a global model (see Fig 6.1), and the inner portion was extracted for crack insertion and remeshing. When the surface effect elements and shear tractions remain with the global model portion, FRANC3D can pass those elements and the loads through to the cracked model.

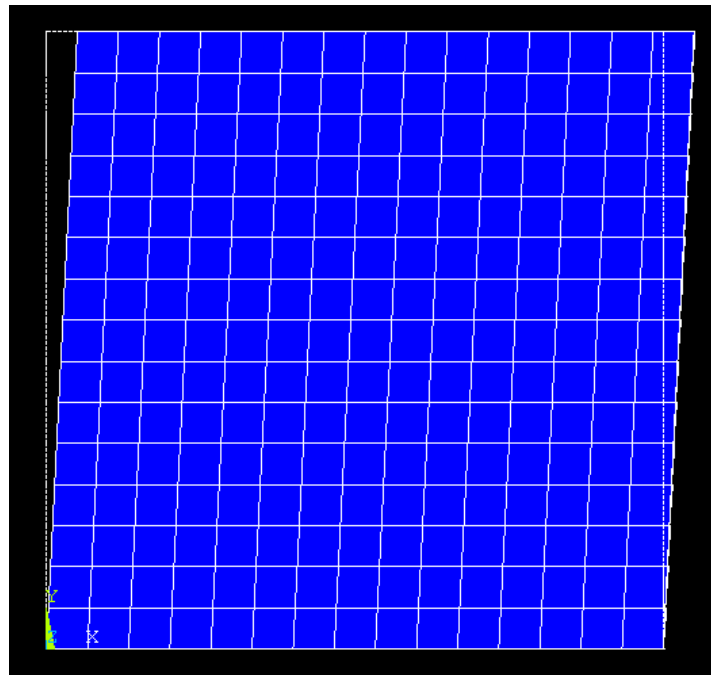


Figure 6.6 Deformed shape under pure shear boundary conditions.

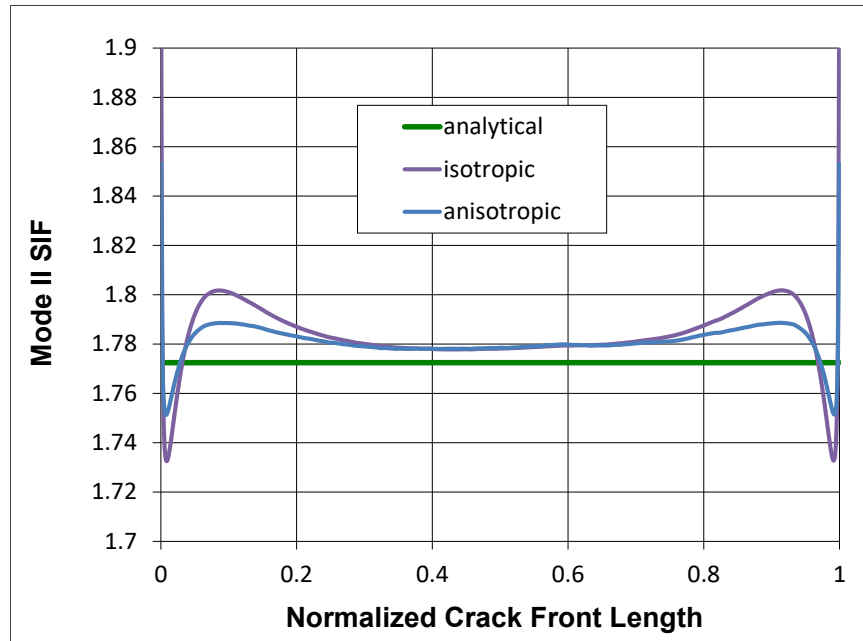


Figure 6.7 SIFs for pure shear for isotropic and anisotropic material properties.

## 7 Corner Crack in a Plate with a Hole

A plate with a corner-cracked hole is another standard benchmark problem. The uncracked plate is 40x40x1 units and has a hole with a radius of 1 unit. Uniform unit tension is applied to the top and bottom surfaces, Fig 7.1. Symmetry boundary conditions are applied so only half of the model is needed.

Symmetry boundary conditions are used, which implies that there will be two symmetric cracks emanating from the hole; this is consistent with the handbook solution. The elastic modulus is set to 10,000 and Poisson's ratio is 0.3.

A quarter-circular corner crack is inserted at the edge of the hole, Fig 7.2; the radius of the crack is 0.1 units. The default crack front template mesh is shown in Fig 7.3; the template radius is 0.01 units. We turn off the Do coarsen... flag for both default and refined template meshes; the default and refined settings are the same as previous models.

About 21,500 elements are generated for the default mesh, and about 64,000 elements are generated for the refined mesh. The deformed shape and the maximum principal stress contours near the corner crack are shown in Fig 7.4.

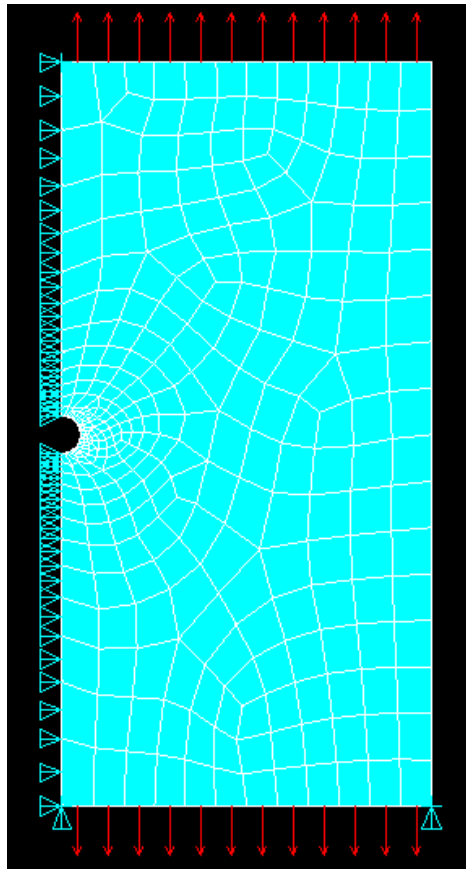


Figure 7.1 Plate with hole under uniform tension in ANSYS.

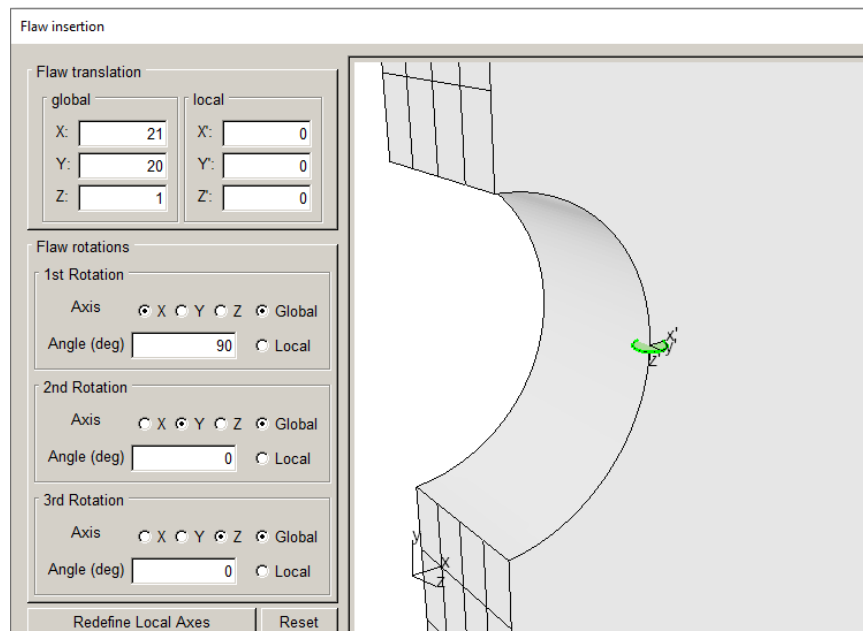


Figure 7.2 Corner crack at the edge of the hole.

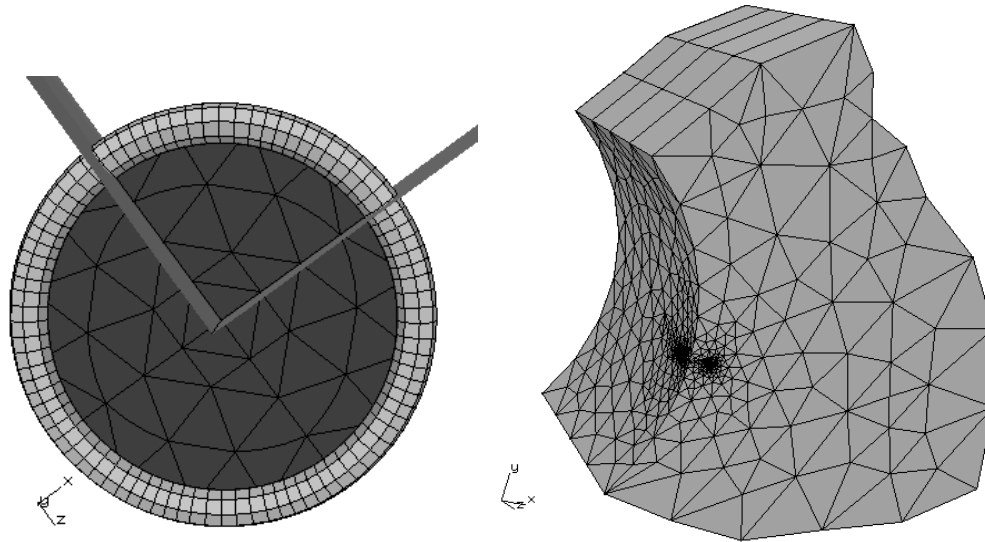


Figure 7.3 Plate with hole and corner crack showing the default template mesh (left) and the resulting cracked remeshed local portion (right).

The stress is higher on the inside of the hole than on the surface of the plate, and the Mode I SIF reflects this, Fig 7.4. The handbook numerical solution is available in Murakami (1987) and from Newman and Raju (1986). The equations from Newman and Raju (1986) have been encoded in Excel and these values are plotted in Fig 7.5. The difference between the computed and handbook values is significant (>10%). Additional reference solutions (Shin, 1990; Lin and Smith, 1999) indicate similar discrepancies with the Newman and Raju (1986) solution for this model.

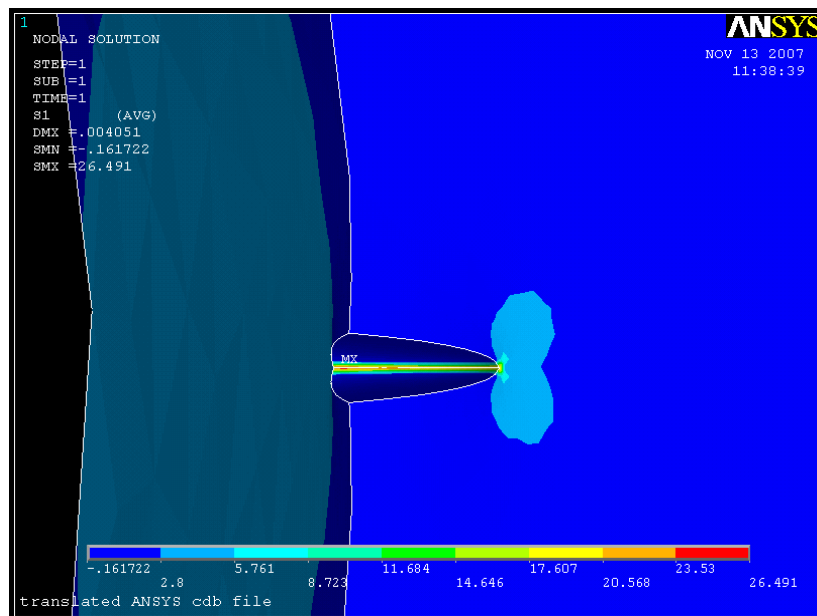


Figure 7.4 Plate with hole and corner crack - deformed shape and maximum principal stress contours.

The Mode I SIF curves for  $Nu=0.0$  are shown in Fig 7.6. Most of the curve matches the handbook solution, but the values at both ends are significantly higher.

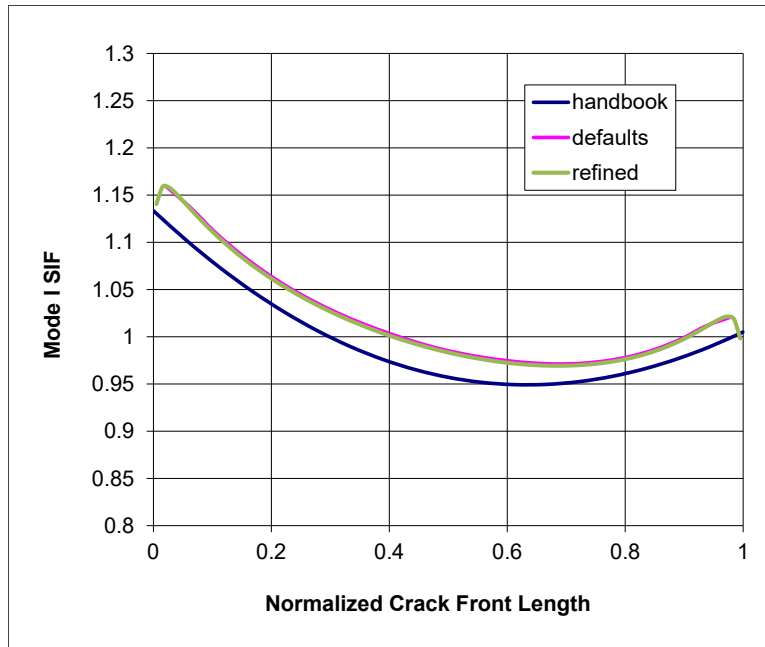


Figure 7.5 Mode I SIF for corner crack in plate with hole; position 0 is inside the hole.

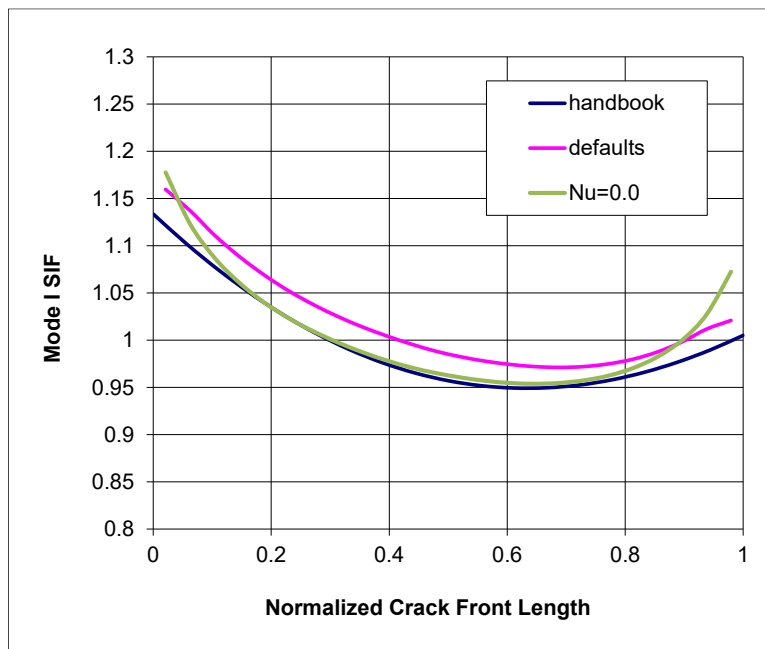


Figure 7.6 Mode I SIF for corner crack in plate with hole for  $Nu=0.0$ .

## 8 Compact Tension Specimen

A compact tension specimen is created in ABAQUS, Fig 8.1. A sketch with relevant dimensions and loads is shown in Fig 8.2. The 2D plane strain equation for  $K_I$  is shown below the sketch. The first equation is based on 1970 work, while the second equation is from Bower (2009) and is considered more accurate.

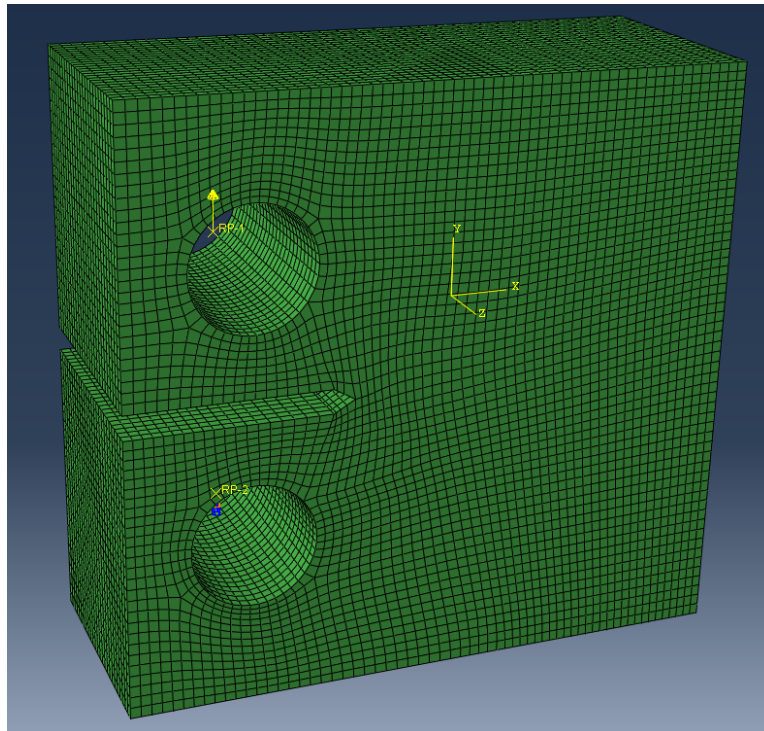
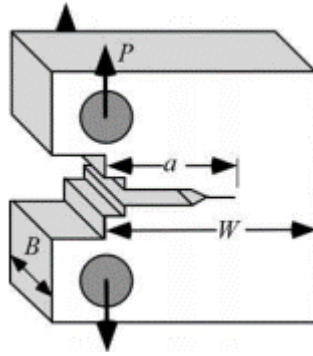


Figure 8.1 Compact tension specimen in ABAQUS.

An edge crack is inserted into a local portion of the FE model; the resulting dimension 'a' is equal to 20 mm. W is 50.4 mm and B is 25.4 mm. Load P is 26358 N. The material properties are set to 20500 and 0.33 for E and  $\nu$ , respectively.

The template radius is set to 0.15, Fig 8.3. This is much smaller than the default radius, which is based on the initial crack dimensions. The Do coarsen... flag can be left on as the crack surface is large. The template parameters are left at their default values.



$$K_I = \frac{\text{LOAD}}{BW^{\frac{3}{2}}} \cdot f\left(\frac{a}{W}\right),$$

where

$$f\left(\frac{a}{W}\right) = \frac{\left(2 + \frac{a}{W}\right) \left\{ 0.886 + 4.64 \left(\frac{a}{W}\right) - 13.32 \left(\frac{a}{W}\right)^2 + 14.72 \left(\frac{a}{W}\right)^3 - 5.6 \left(\frac{a}{W}\right)^4 \right\}}{\left(1 - \frac{a}{W}\right)^{\frac{3}{2}}}$$

$$K_I = \frac{P}{B} \sqrt{\frac{\pi}{W}} \left[ 16.7 \left(\frac{a}{W}\right)^{1/2} - 104.7 \left(\frac{a}{W}\right)^{3/2} + 369.9 \left(\frac{a}{W}\right)^{5/2} - 573.8 \left(\frac{a}{W}\right)^{7/2} + 360.5 \left(\frac{a}{W}\right)^{9/2} \right]$$

Figure 8.2 Compact tension SIF equations.

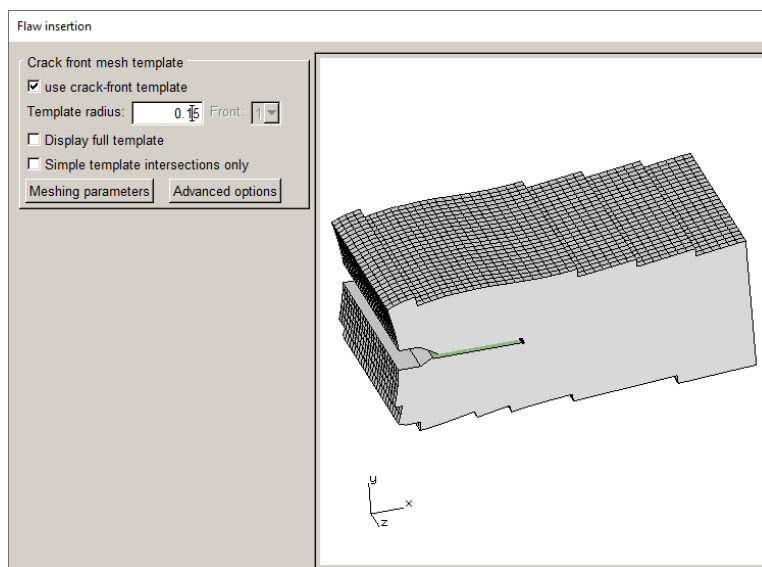


Figure 8.3 Local model portion with edge crack template radius set to 0.15.

The FRANC3D values for the Mode I SIF are shown in Figure 8.4. As in Section 5, it is clear that the model is not in plane strain or plane stress. To simulate the conditions of plane strain, we set the Poisson's ratio to 0.0 and redo the analysis. The result is a 'constant' value for  $K_I$  along the crack front, Fig 8.5. The average value is 1063.6, and the second equation in Fig 8.2 gives a value of 1058.3  $\text{MPa}\sqrt{\text{mm}}$ ; the difference is 0.5%

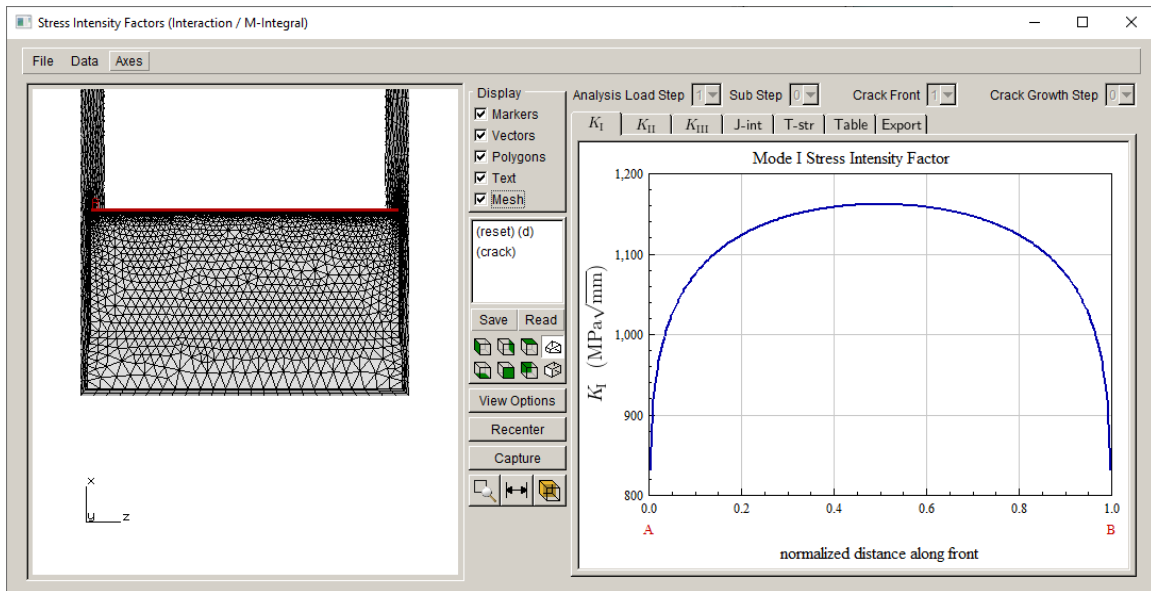


Figure 8.4 Compact tension Mode I SIF with  $\nu=0.33$ .

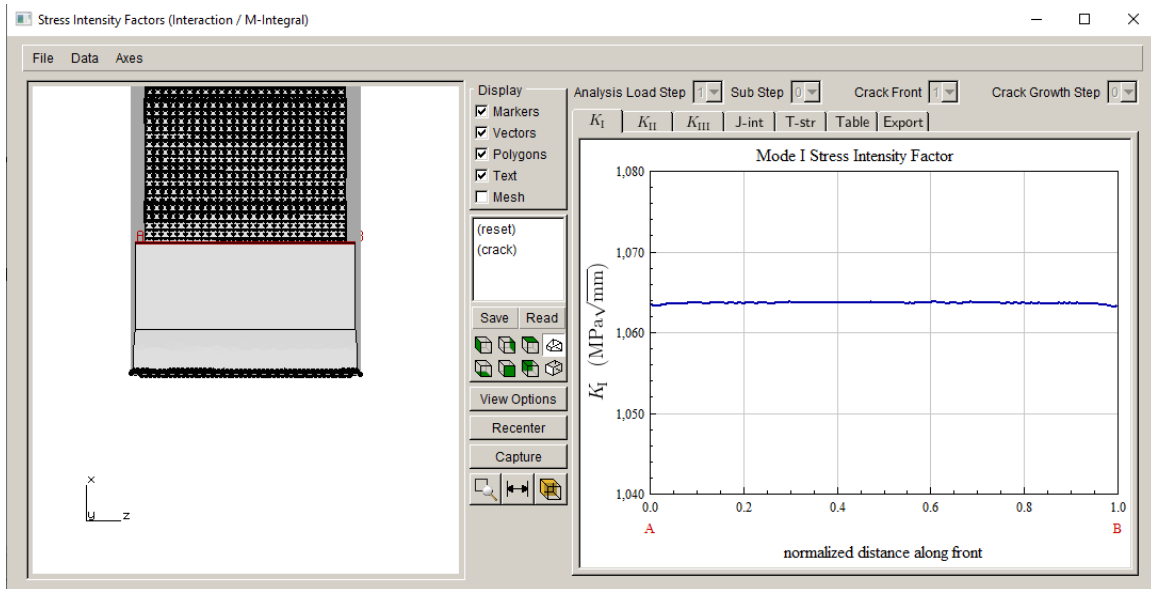


Figure 8.5 Compact tension Mode I SIF with  $\nu=0$ .

Rather than setting Poisson's ratio to zero, z-constraints could be added to the 'front' and 'back' surfaces of the model to simulate plane strain, as was done in Section 5. The resulting SIFs should be 'constant' and match the above SIFs for  $\nu=0$ ; this is left as an exercise for the reader.

## 9 Circumferential Cracked Rod

A solid rod is created in ABAQUS, Fig 9.1. A sketch with relevant dimensions and loads is shown in Fig 9.2. The loading is far-field uniform unit tension normal to the crack surface. The material properties consist of an elastic modulus of 1000 and a Poisson's ratio of 0.3.

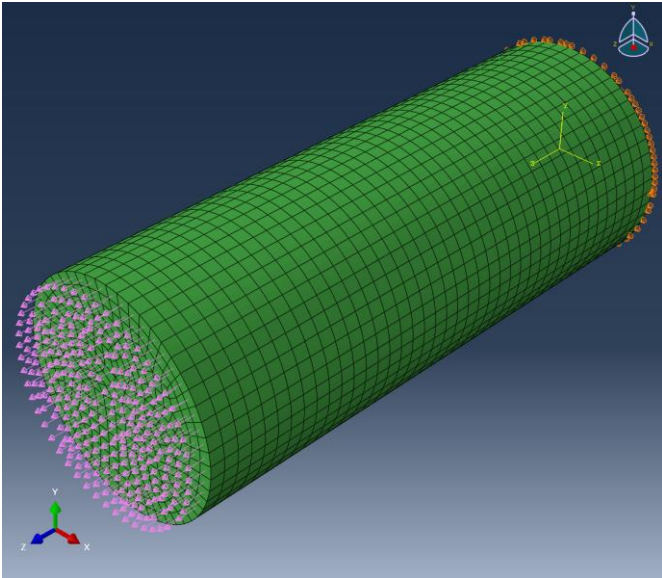


Figure 9.1 Solid rod model in ABAQUS.

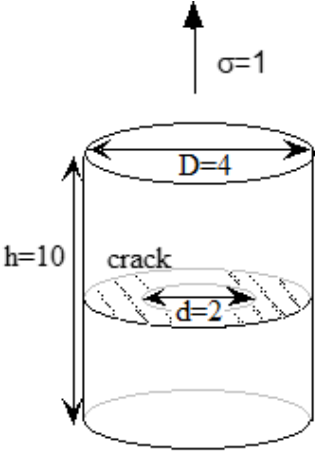


Figure 9.2 Solid rod dimensions.

The handbook solution for the Mode I SIF for this type of crack is given in Murakami (page 643) as:

$$F_I^* = \frac{K_I}{0.5 \sigma_{net} \sqrt{\pi d/2}}$$
$$\sigma_{net} = \left(\frac{D}{d}\right)^2 \sigma$$

Figure 9.3 Circumferential crack SIF equations.

For the bar and crack dimensions given above, the correction factor,  $F_I^*$ , for a Poisson ratio of 0.3 is taken from the graph in Murakami to be 0.97, which then gives a value for  $K_I$  of 3.44.

The FRANC3D crack mesh, Fig 9.4, has a template radius of 0.05 units. The mode I SIFs are shown in Fig 9.5. The average value is 3.42, and the average difference from the handbook value is 0.5%.

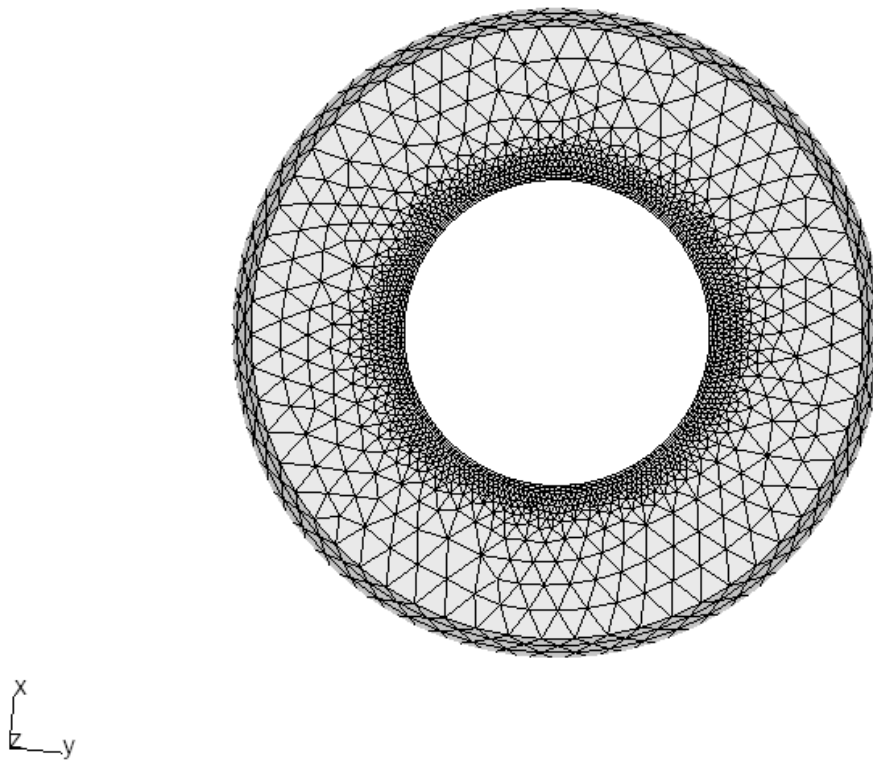


Figure 9.4 Circumferential crack surface mesh.

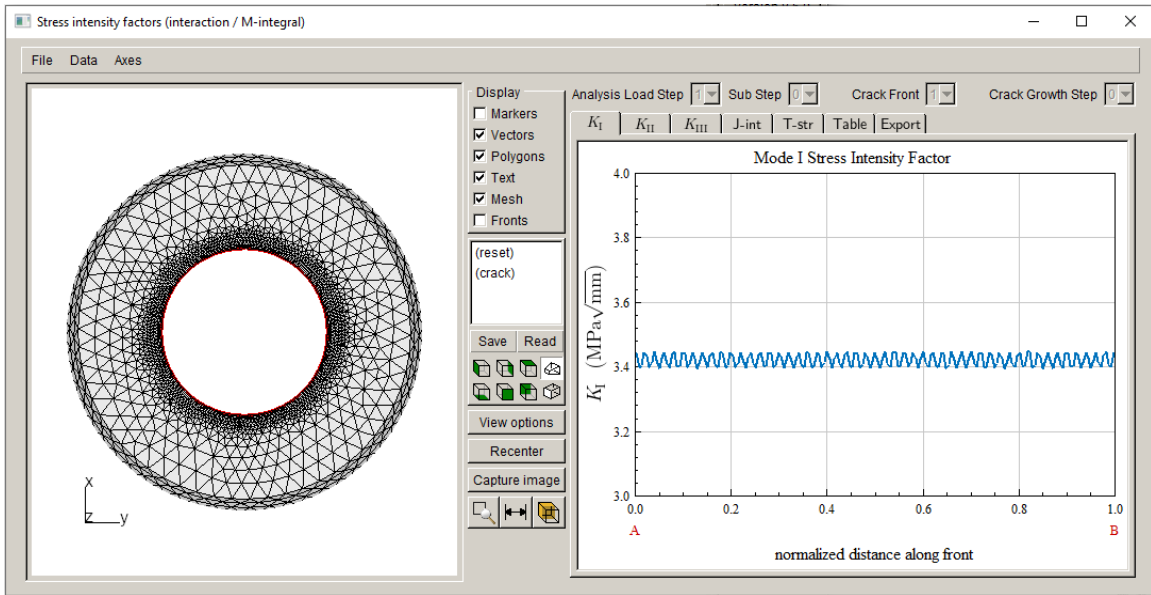


Figure 9.5 Circumferential crack surface mesh.

## 10 Transverse Crack in a Pipe

A pipe is created in ABAQUS, Fig 10.1. A sketch with relevant dimensions and loads is shown in Fig 10.2. The loading is far-field uniform unit tension normal to the crack surface. The material properties consist of an elastic modulus of  $1e7$  and a Poisson's ratio of 0.33.

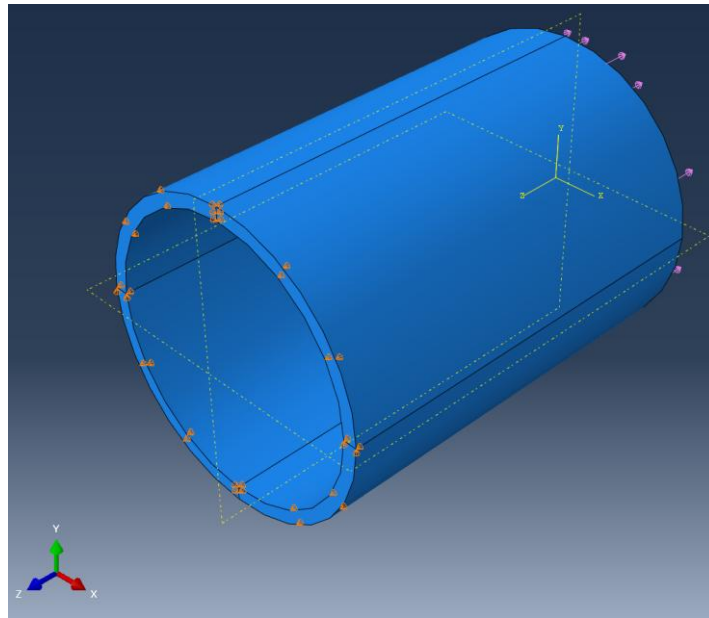


Figure 10.1 Pipe model in ABAQUS.

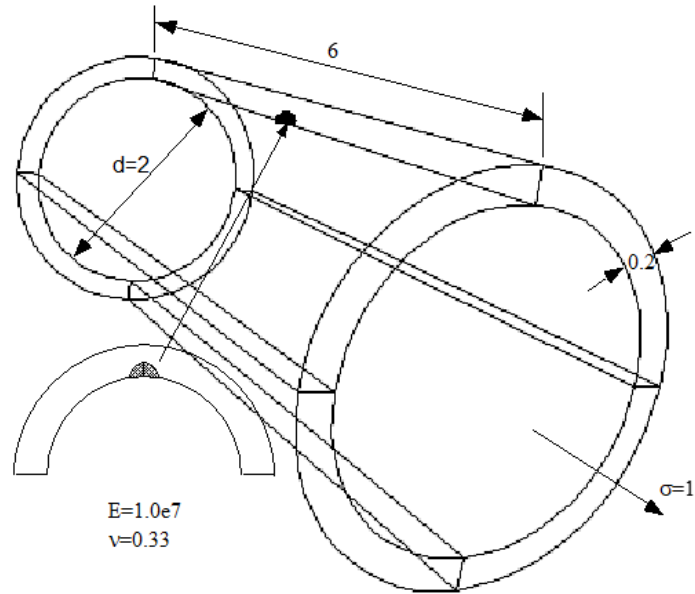


Figure 10.2 Pipe model dimensions.

A half-penny transverse crack with a radius of 0.08 is placed in the pipe on the interior surface, centered with respect to the pipe length. The crack surface mesh is shown in Fig 10.3 for a template radius of 0.005 units.

The handbook solution is available from several sources (*e.g.*, Bergman, 1995). The Mode II and III SIFs are zero. The minimum value of mode I SIF occurs at the deepest part of the crack and is equal to 0.341, while the maximum occurs where the crack front meets the inner pipe surface and is equal to 0.388. The accuracy of the reference values is not given.

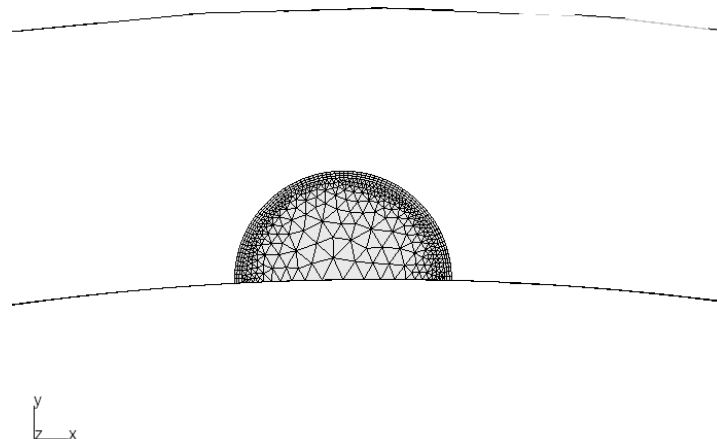


Figure 10.3 Pipe - transverse crack surface mesh.

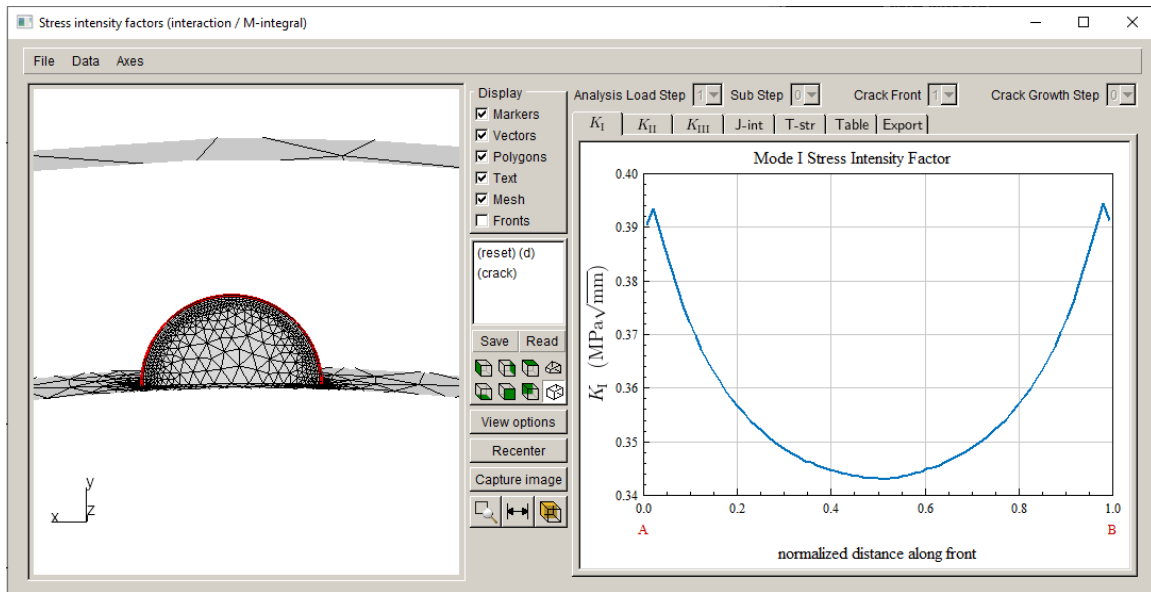


Figure 10.4 Pipe - transverse crack Mode I SIFs.

The minimum Mode I SIF in Fig 10.4 is 0.343, which is basically the same as the reference solution.

## 11 Summary

The benchmark model files can be downloaded from the FAC website.

Additional benchmark models can be found in Murakami (1987) or in fracture mechanics texts, such as Anderson (1991).

We have not provided any benchmarks for fatigue-life (cycle) counts. Tutorial #6 (see the Tutorials 2-14 document) describes a typical fatigue test specimen and the corresponding FRANC3D simulation; that example is intended to simply be a tutorial to describe how one could benchmark the fatigue life computations.

## References

- Anderson, T.L. (1991) *Fracture Mechanics Fundamentals and Applications*, CRC Press.
- Banks-Sills, L., Hershkovitz, I., Wawrzynek, P.A., Eliasi, R., and Ingraffea, A.R. (2005) Methods for calculating stress intensity factors in anisotropic materials: Part I— $z = 0$  is a symmetric plane”, *Eng Fract Mech*, 72, 2328–2358.
- Banks-Sills, L., Wawrzynek, P.A., Carter, B.J., Ingraffea, A.R. and Hershkovitz, I. (2007) Methods for calculating stress intensity factors in anisotropic materials: Part II—Arbitrary geometry, *Eng Fract Mech*, Vol 74, No 8, pp 1293-1307.
- Bergman, M. (1995) Stress Intensity Factors for Circumferential Surface Cracks in Pipes, *Fatigue Fract. Engng. Mater. Struct.*, 18, 10, pp 1155-1172.
- Bower, A. F. (2009). *Applied mechanics of solids*. CRC Press.
- Lin, X.B and Smith, R.A. (1999) Stress intensity factors for corner cracks emanating from fastener holes under tension, *Eng Fract Mech*, 62, 535-553.
- Murakami, Y. (Editor-in-Chief), *Stress Intensity Factors Handbook*, Pergamon Press, 1987.
- Newman, J.C. and Raju, I.S. (1986) Stress-Intensity Factor Equations for Cracks in Three-Dimensional Finite Bodies Subjected to Tension and Bending Loads, Chapter 9, *Computational Methods in the Mechanics of Fracture*, Edited by S.N. Atluri, Elsevier Science Publishers, p. 311-334.
- Raju, I. S., Newman, J. C. (1979) Stress-intensity factors for a wide range of semi-elliptical surface cracks in finite thickness plates, *Eng Fract Mech.*, 11, 817-829.
- Shin, C.S. (1990) The stress intensity of corner cracks emanating From Holes, *Eng Fract Mech*, 7, p423-436.